Electronic Supplementary Material (ESI) for New Journal of Chemistry.
This journal is © The Royal Society of Chemistry and the Centre National de la Recherche Scientifique 2018

Fabrication of Amine and imine-functionalized Isoreticular Pillared-layer Metal-Organic Frameworks for Highly Selective Detection of Nitro-aromatics

Somayeh Tarasi,[†] *Alireza Azhdari Tehrani,*[†] *Ali Morsali,*[*†] *Pascal Retailleau*[‡]

[†]*Department of Chemistry, Faculty of Sciences, Tarbiat Modares University, P.O. Box: 14115-175, Tehran, Iran. E-mail: Morsali_a@modares.ac.ir*

[‡]*CNRS UPR 2301, Institut de Chimie des Substances Naturelles, Univ. Paris-Sud, Université Paris-Saclay, 1, av. de la Terrasse, 91198 Gif-sur-Yvette, France*

Experimental Section

Materials and Physical Techniques

All starting materials, including Zinc (II) nitrate hexahydrate 1, 1'-Carbonyldiimidazole, 4, 4'-oxybis (benzoic acid) (H_2OBA) were purchased from Aldrich and Merck Company and used as received. Melting points were measured on an Electrothermal 9100 apparatus. FT-IR spectra were recorded using Thermo Nicolet IR 100 FT-IR. The thermal behavior was measured with a PL-STA 1500 apparatus with the rate of 10ºC.min^{-1} in a static atmosphere of argon. X-ray powder diffraction (XRD) measurements were performed using a Philips X'pert diffractometer with mono chromated Cu-Kα radiation. The ^{1}H-NMR spectrum was recorded on a Bruker AC-250 MHz spectrometer at ambient temperature in d_6- DMSO and D_2SO_4. The samples were also characterized by field emission scanning electron microscope (FE-SEM) SIGMA ZEISS and TESCAN MIRA with gold coating.

X-ray crystallography analysis

Single crystals of TMU-6(RL1) and TMU-21(RL2) were selected and mounted on a loop in inert oil and transferred to the cold gas stream of a Bruker APEX-II CCD diffractometer. The data was corrected for absorption and beam corrections based on the multi-scan technique as implemented in *SADABS*. The structures were solved by conventional methods and refined by full-matrix least-squares on all F^2 data using SHELX97 or SHELX2014 in conjunction with the X-Seed or Olex2 graphical user interface. Anisotropic thermal parameters were refined for non-hydrogen atoms and hydrogen atoms were calculated and refined with a riding model.

Crystallographic data: TMU-6(RL1): $C_{23}H_{17}N_2O_5Zn$, M= 466.75 g mol^{-1}, Monoclinic, C2/C, a= 14.953(6) Å, b= 23.994(9) Å, c= 15.975(6) Å, β= 112.674(2), V= 5289.2(4) Å^3, Z=8, ρ_{calc}= 1.172 g cm^{-3}, λ= 1.54178, T=100 K, R_1= 0.0306, wR_2= 0.0848, S= 1.049, ccdc= 1814568

Crystallographic data: TMU-21(RL2): $C_{25}H_{18}N_2O_5Zn$, M= 564.88 g mol^{-1}, Monoclinic, C2/C, a= 14.656(9) Å, b= 25.332(10) Å, c= 15.943(8) Å, β= 109.865(6), V= 5567.1(5) Å^3, Z=8, ρ_{calc}= 1.348 g cm^{-3}, λ= 0.71073, T=293 K, R_1= 0.0428, wR_2= 0.1110, S= 1.015, ccdc= 1814569

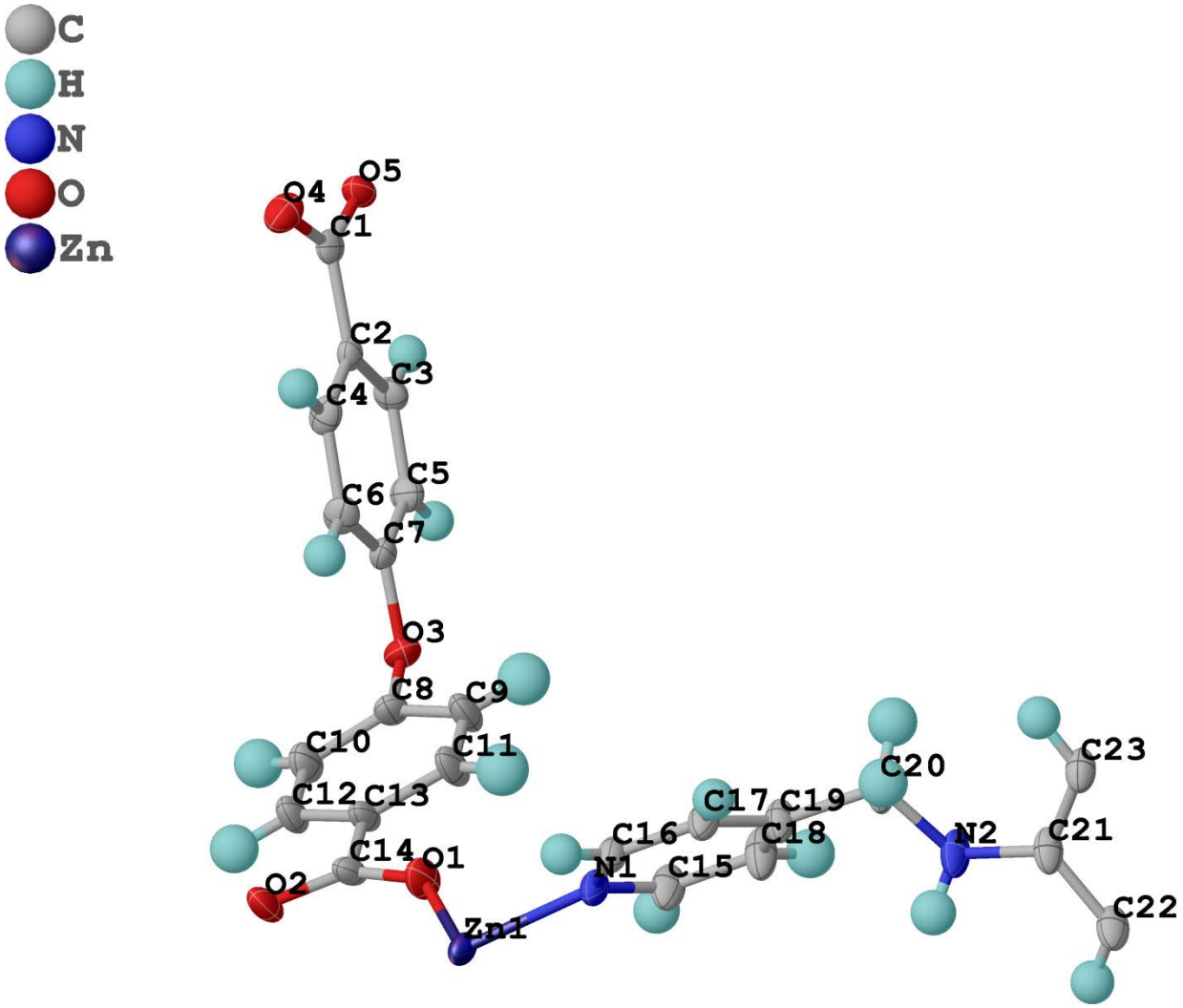

Figure S1. Binuclear Secondary Building Unit in **TMU-6(RL1)**

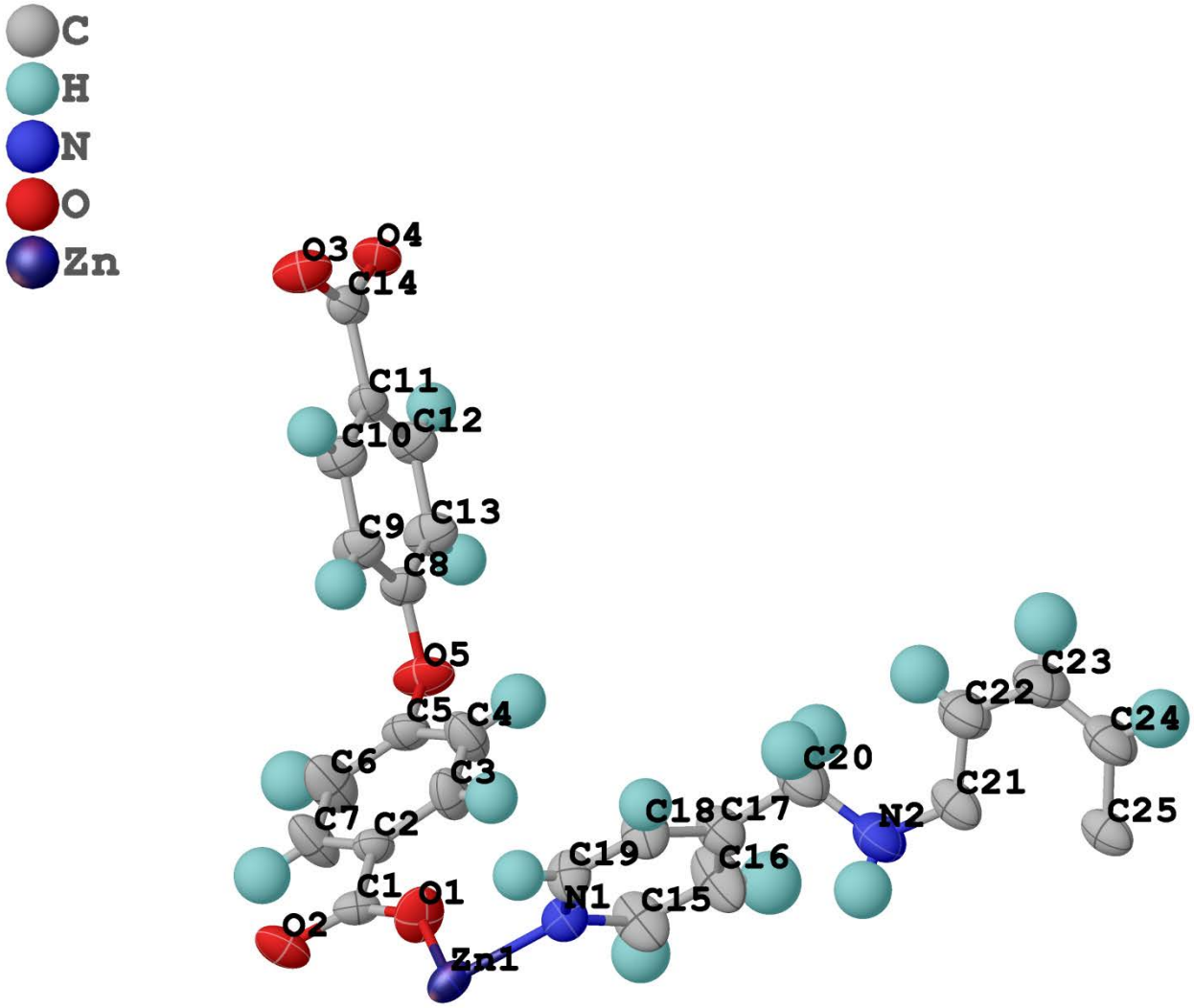

Figure S2. Binuclear Secondary Building Unit in **TMU-21(RL2)**

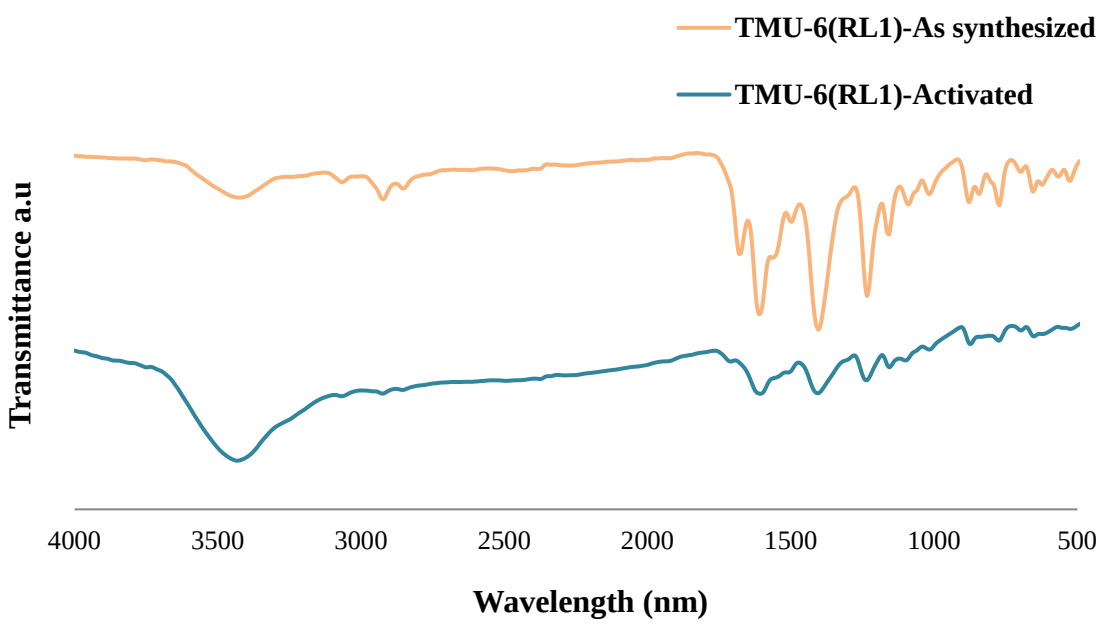

Figure S3. FT-IR spectra of **TMU- 6(RL1)**

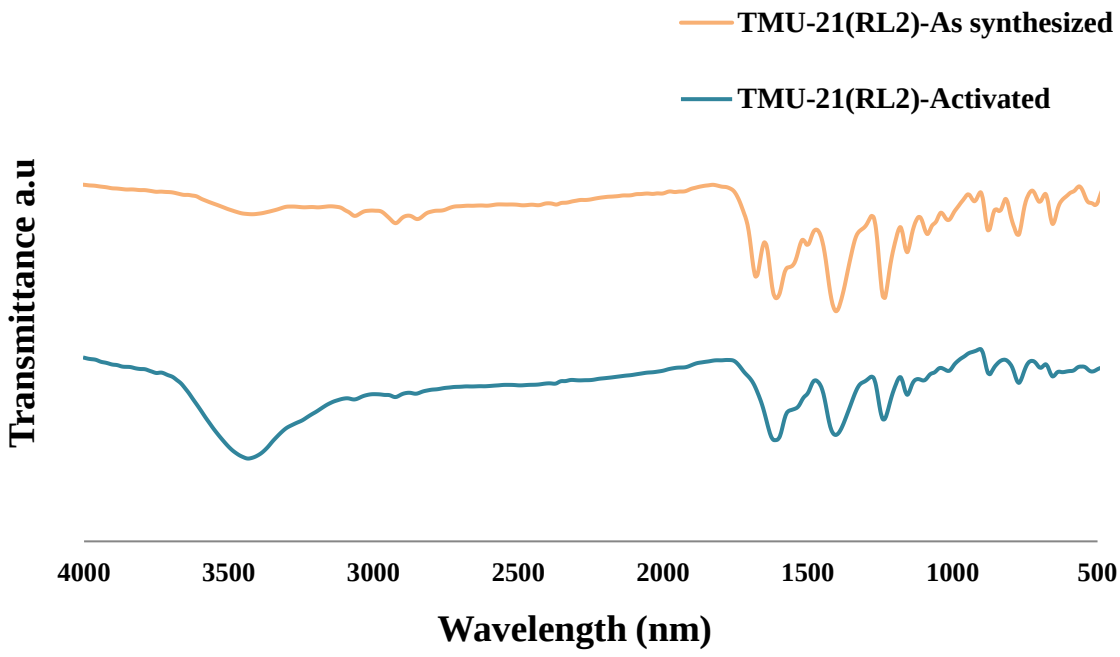

Figure S4. FT-IR spectra of **TMU- 21(RL2)**

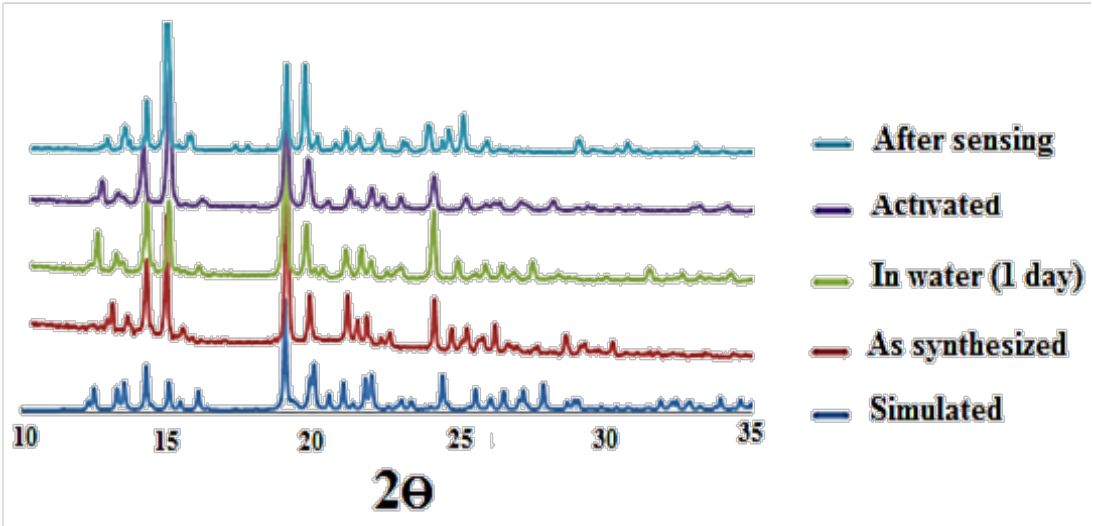

Figure S5. PXRD patterns of simulated, as-synthesized, stabilities in water solvent, after Sensing and activated form of **TMU-6(RL1)**

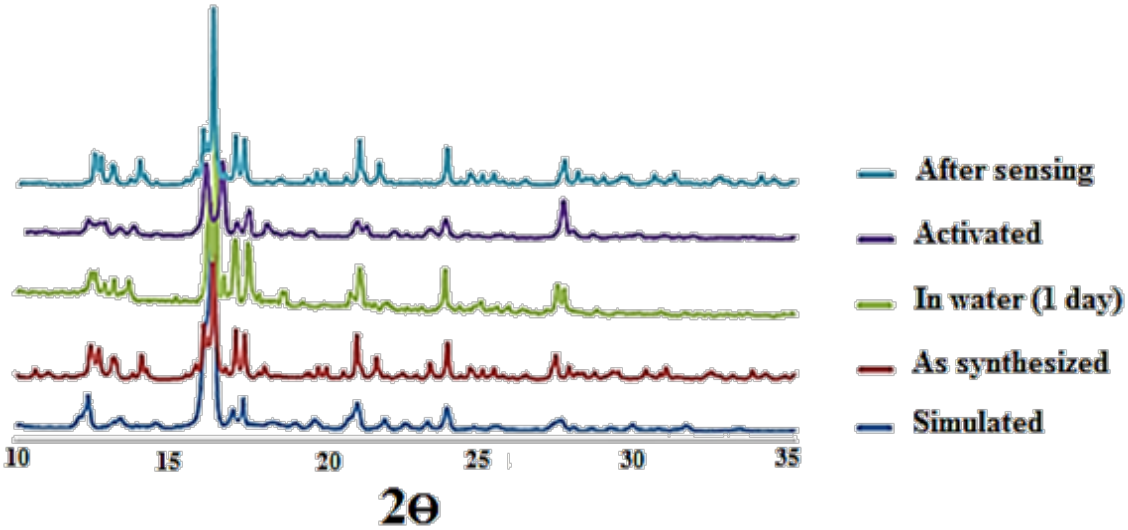

Figure S6. PXRD patterns of simulated, as-synthesized, stabilities in water solvent, after Sensing and activated form of **TMU-21(RL2)**

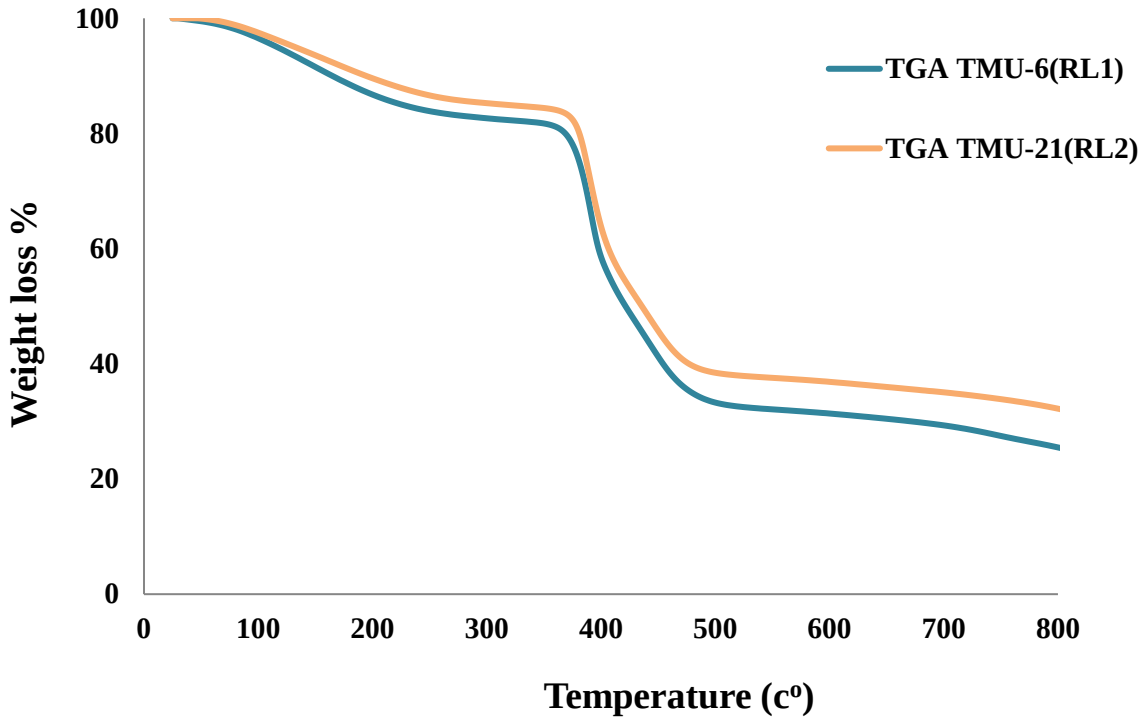

Figure S7. Thermogravimetric analysis of **TMU-6(RL1)** and **TMU-21(RL2)**

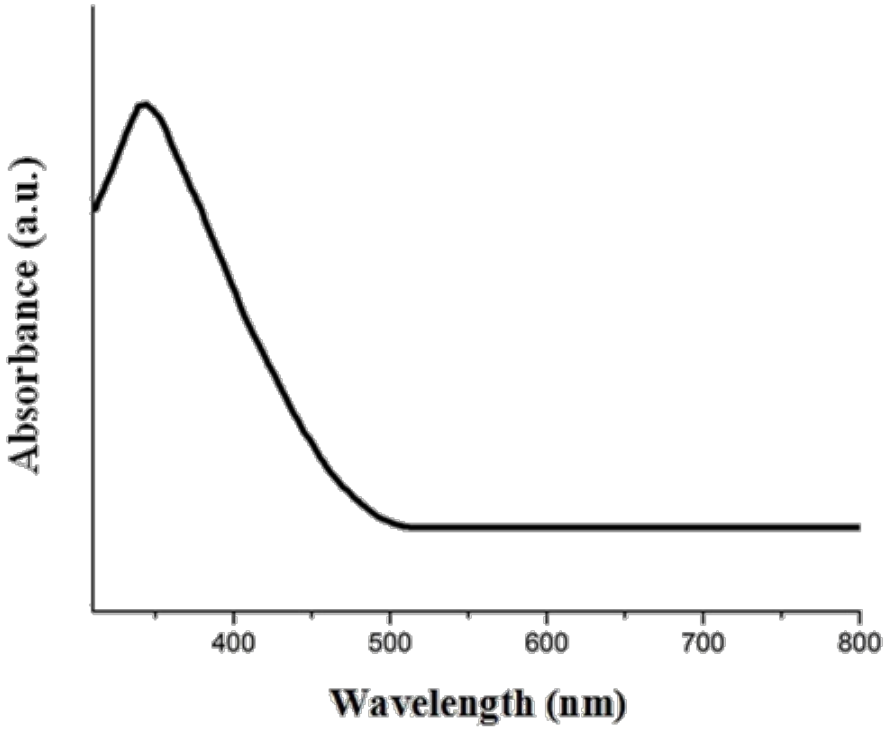

Figure S8. Solid state UV-vis spectroscopy of **TMU-6(L1)**

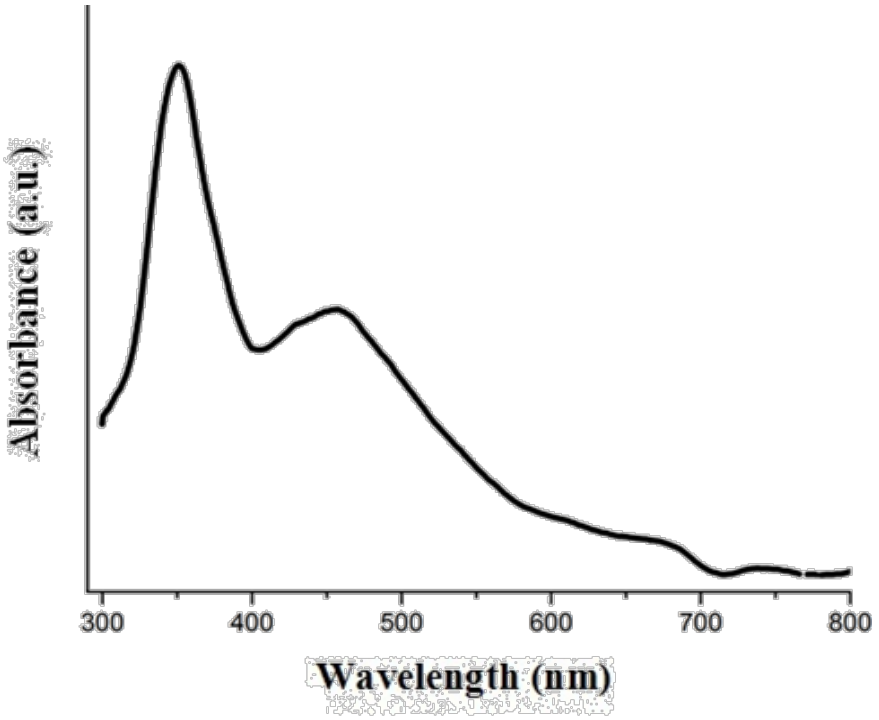

Figure S9. Solid state UV-vis spectroscopy of **TMU-21(L2)**

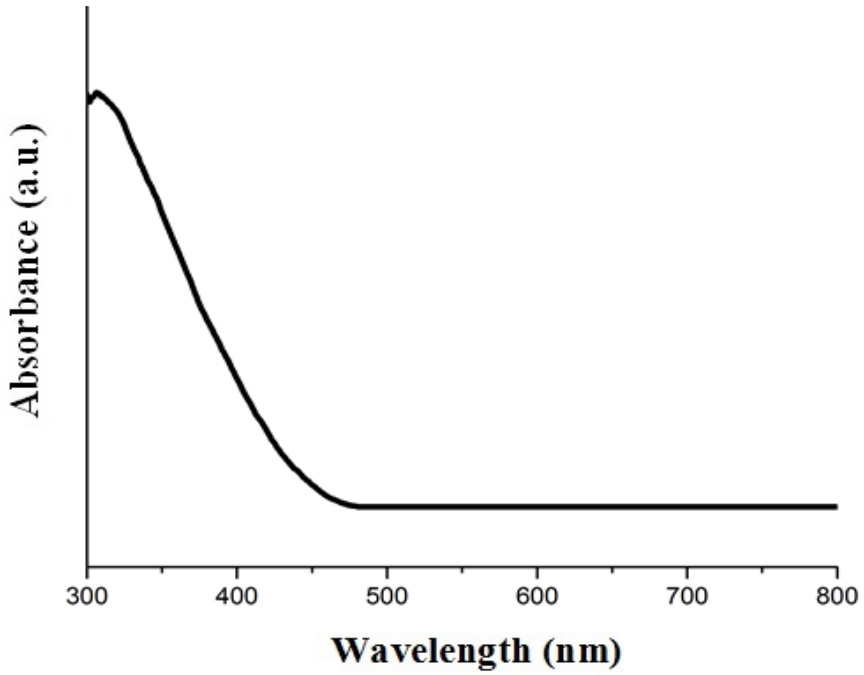

Figure S10. Solid state UV-vis spectroscopy of **TMU-6(RL1)**

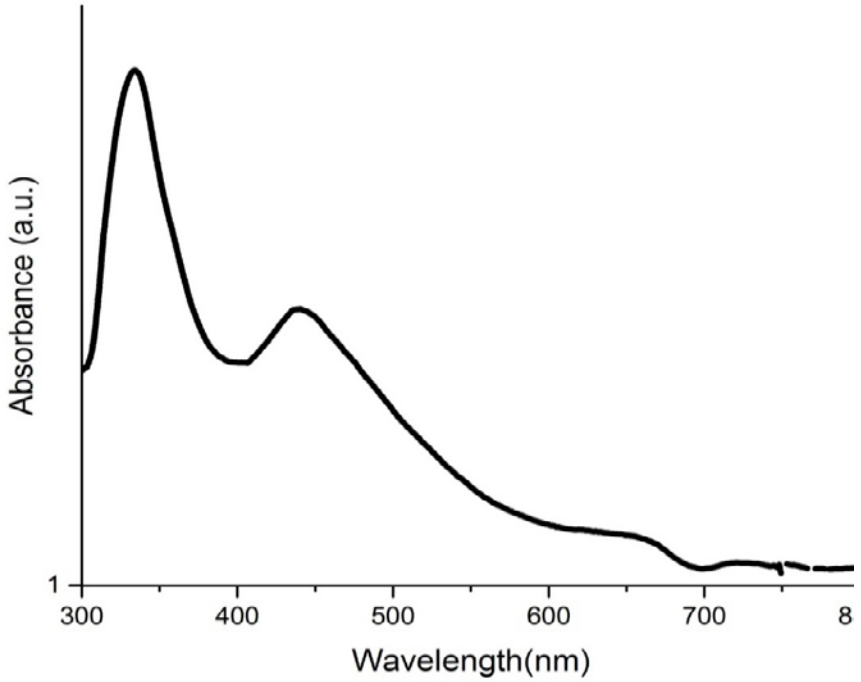

Figure S11. Solid state UV-vis spectroscopy of **TMU-21(RL2)**

Fluorescence Measurements

The Fluorescence properties of TMU-6(RL1) and TMU-21(RL2) were measured in different solvent emulsions containing MOF using a PerkinElmer-LS55 fluorescence spectrometer at room temperature. In a typical procedure, 2 mg of an activated MOF was grinded down, and then immersed in different analyte a solution (3 ml) was tested in the emission mode. For fluorescence measurement in the presence of nitroaromatic compounds toluene was chosen as suitable solvent.

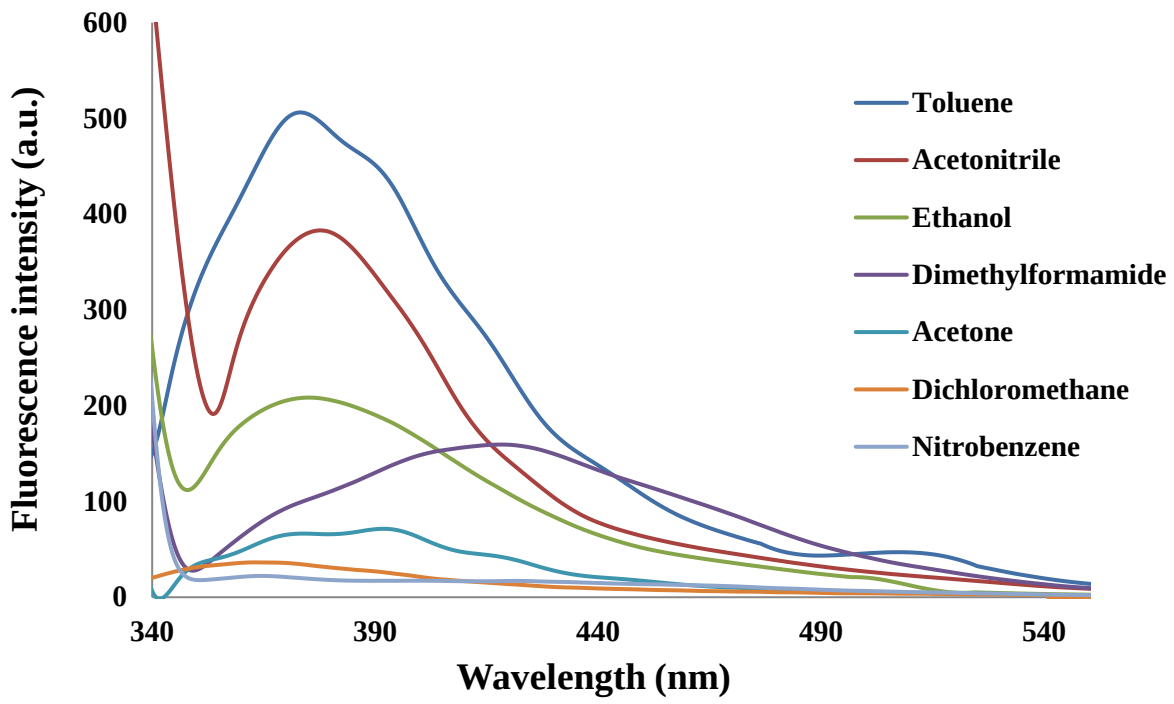

Figure S12. Fluorescence emission spectra of **TMU-6(RL1)** dispersed in different solvents

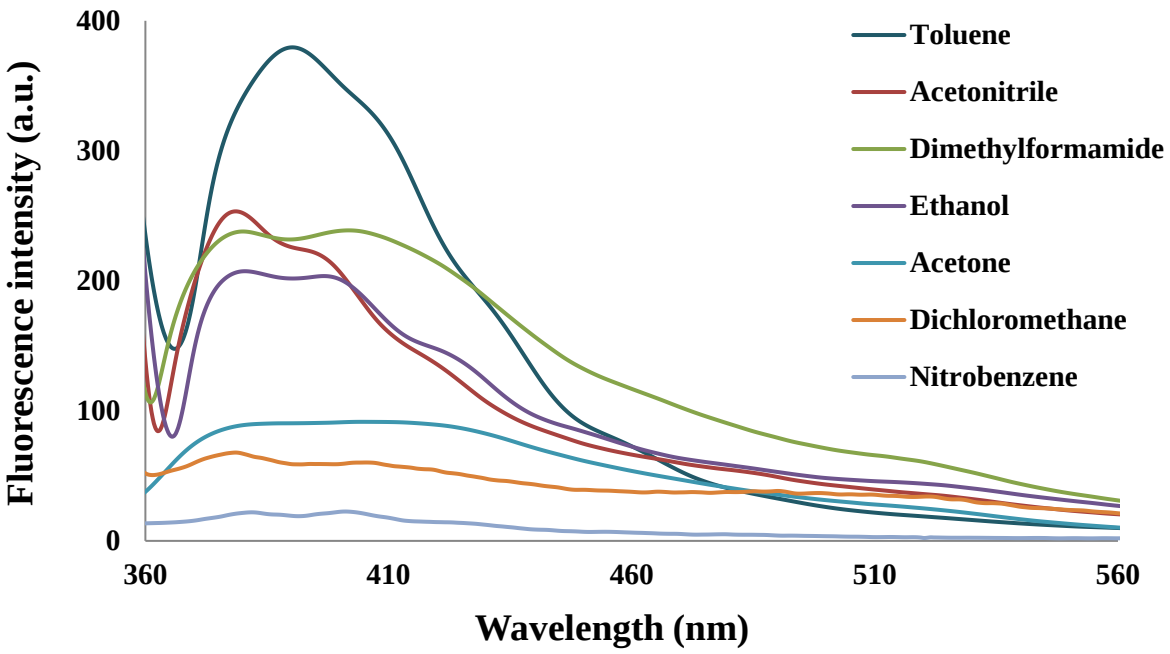

Figure S13. Fluorescence emission spectra of **TMU-21(RL2)** dispersed in different solvents

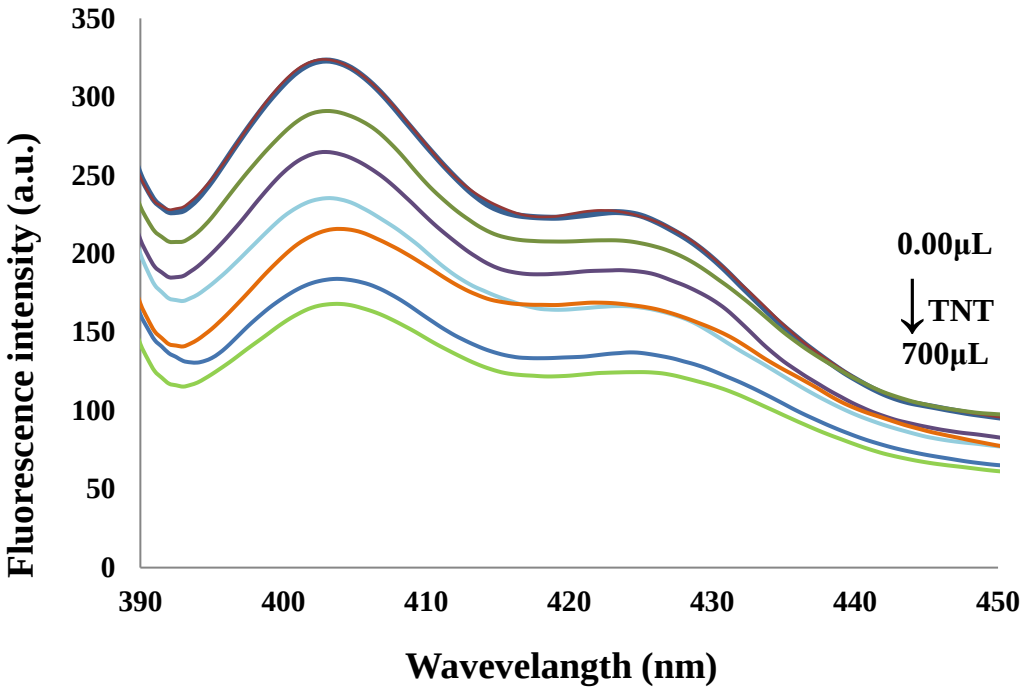

Figure S14.Fluorescence emission spectra of **TMU-6(L1)** dispersed in toluene solution at different concentrations of **TNT**.

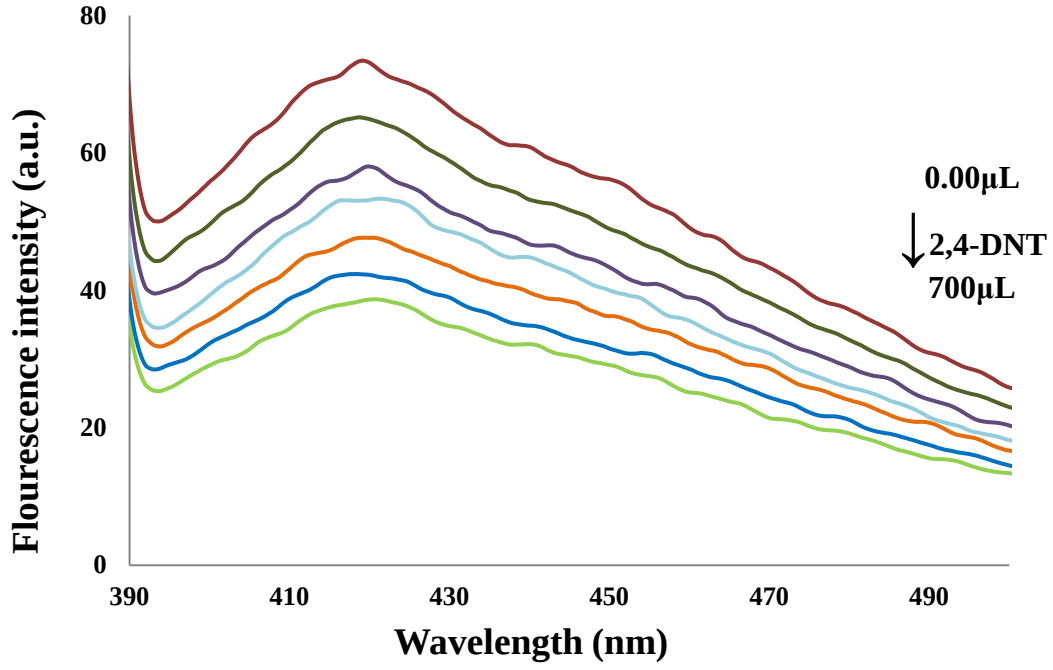

Figure S15.Fluorescence emission spectra of **TMU-6(L1)** dispersed in toluene solution at different concentrations of **2,4-DNT.**

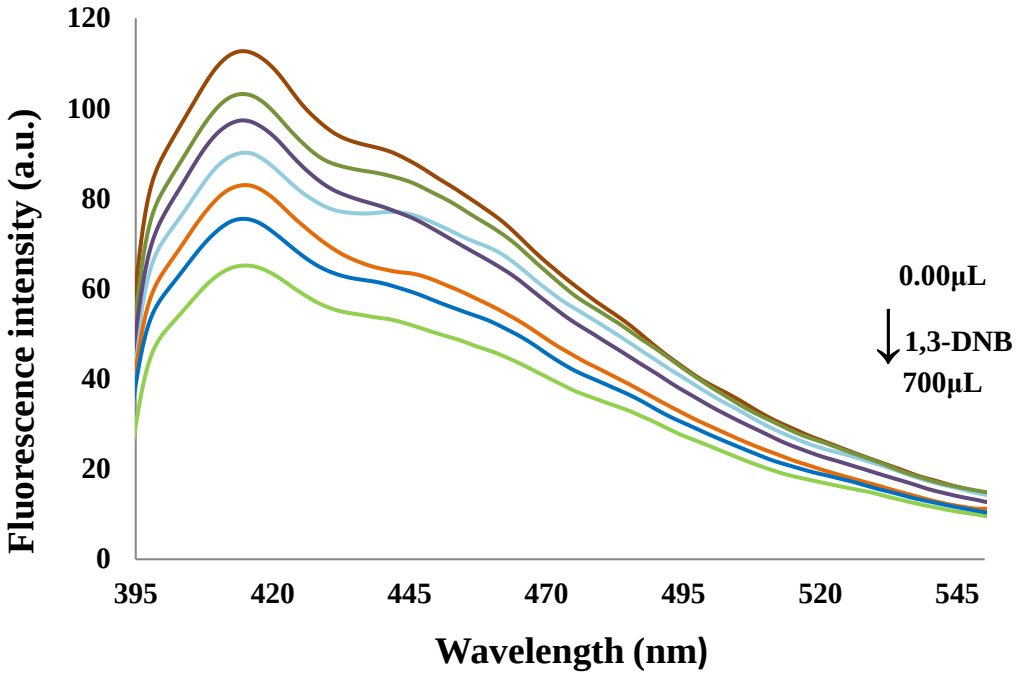

Figure S16.Fluorescence emission spectra of **TMU-6(L1)** dispersed in toluene solution at different concentrations of **1,3-DNB**

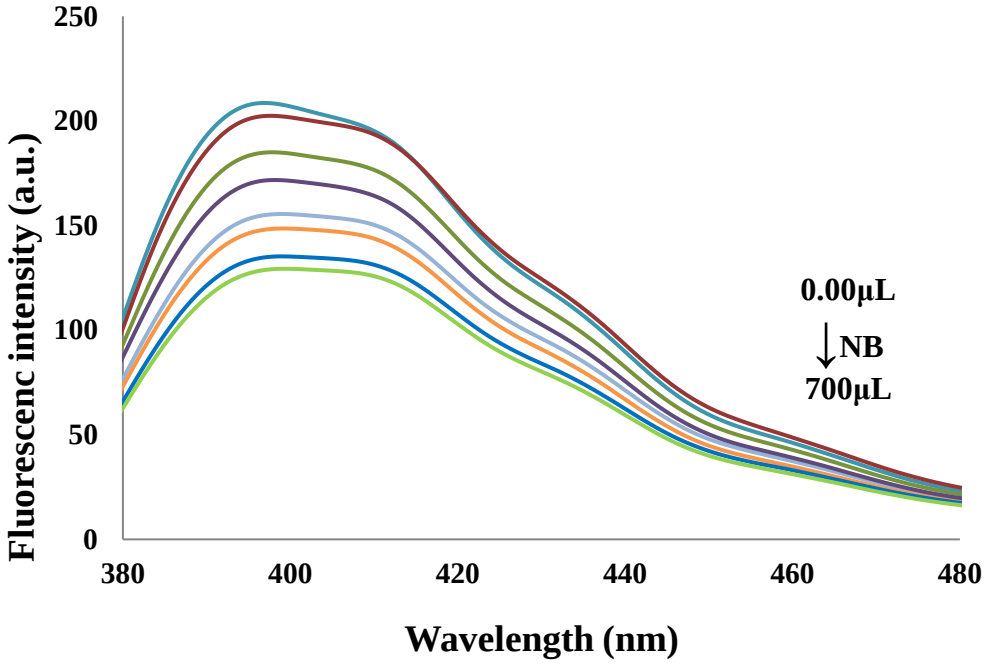

Figure S17.Fluorescence emission spectra of **TMU-6(L1)** dispersed in toluene solution at different concentrations of **NB**

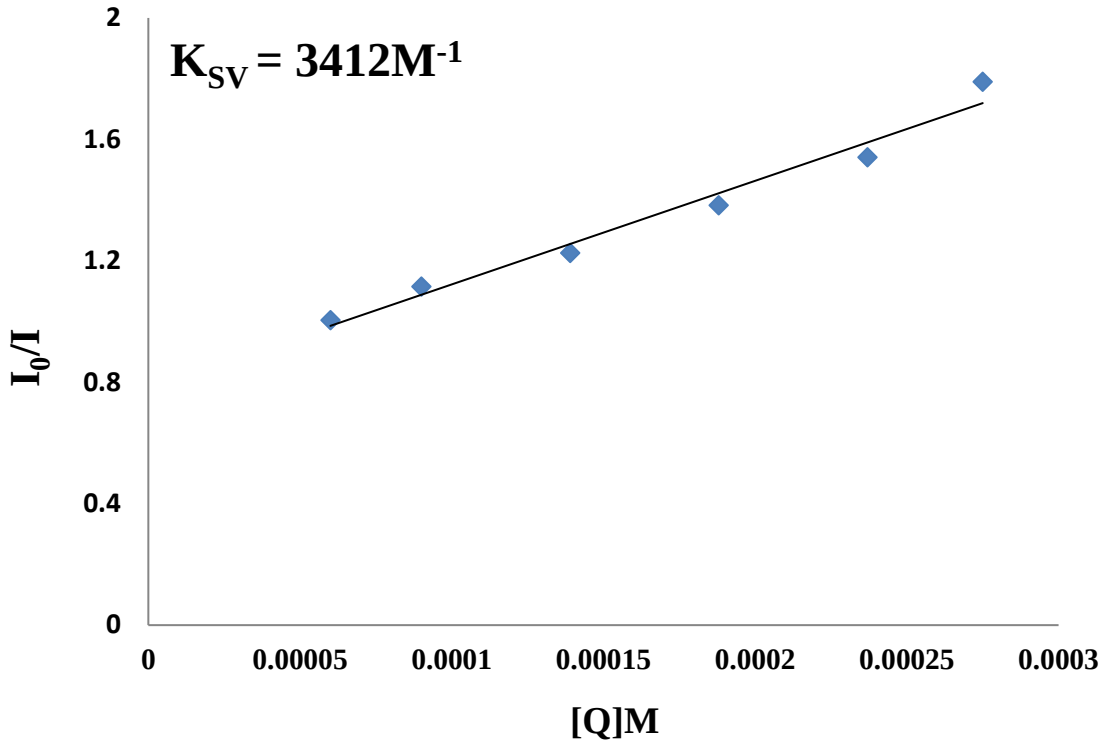
K_{SV} = 3412M^{-1}
2
1.6
1.2
0.8
0.4
0
I_0/I
0
0.00005
0.0001
0.00015
0.0002
0.00025
0.0003
[Q]M

(a)

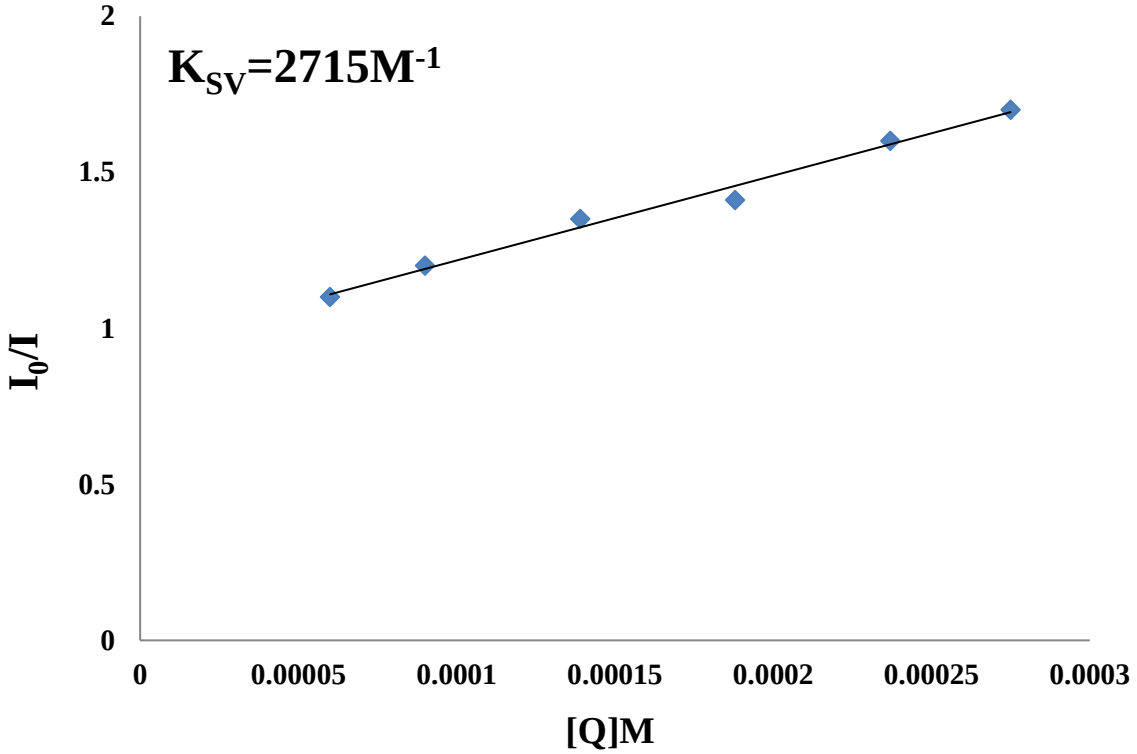
K_{SV}=2715M^{-1}
2
1.5
1
0.5
0
I_0/I
0
0.00005
0.0001
0.00015
0.0002
0.00025
0.0003
[Q]M

(b)

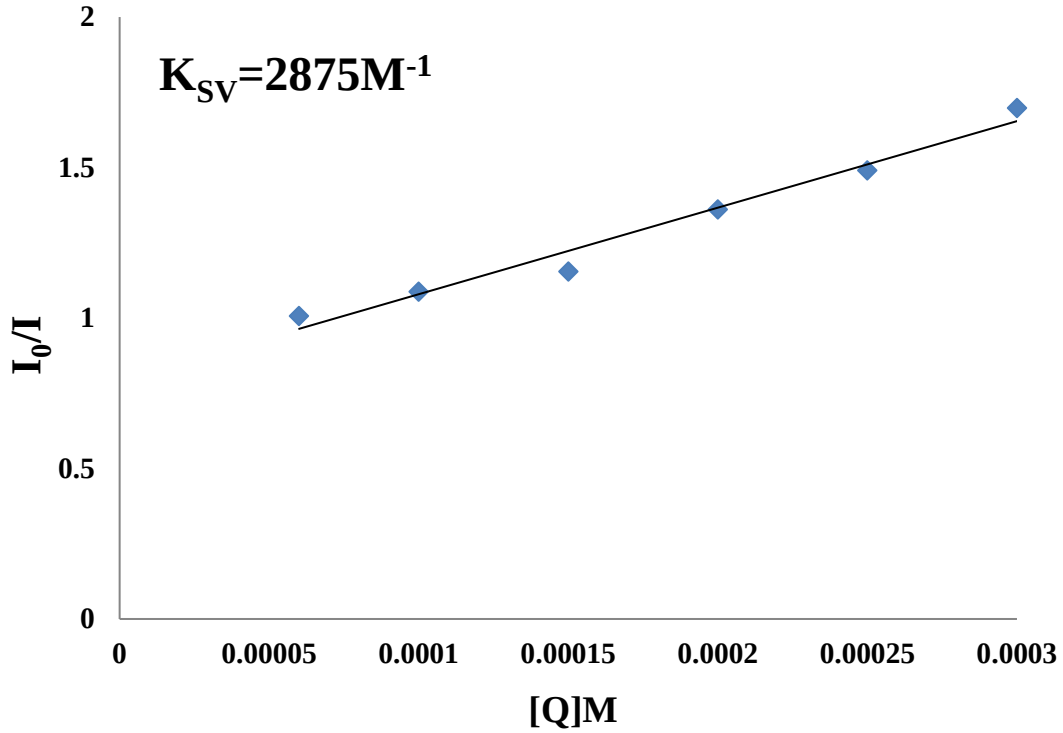

(c)

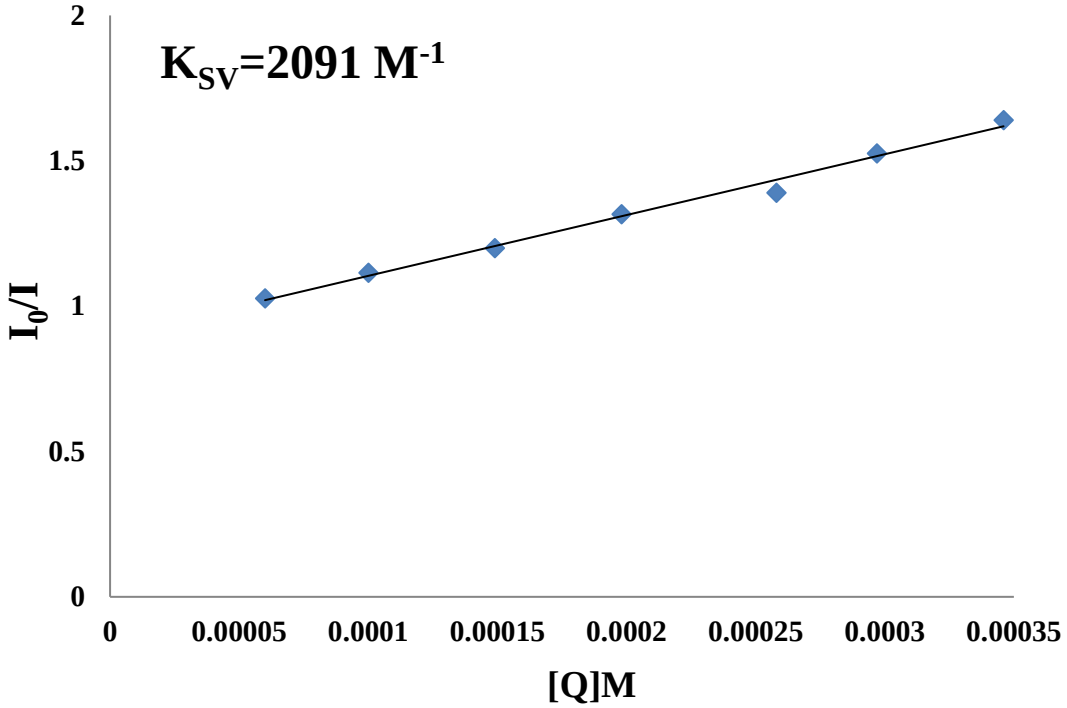

(d)

Figure S18.Stern -Volmer (SV) plots in the presence of 2 mg of **TMU-6(L1)** in different **TNT** (a) **2,4-DNT** (b) **1,3-DNB** (c) **NB** (d) concentrations ([Q]) in toluene

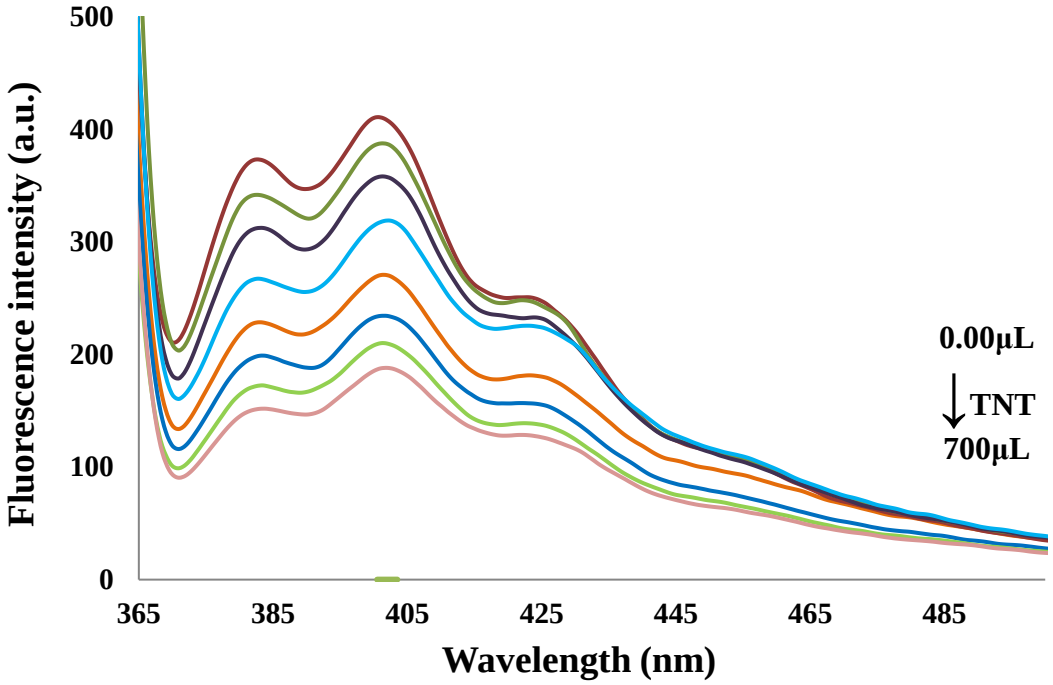

Figure S19.Fluorescence emission spectra of **TMU-21(L2)** dispersed in toluene solution at different concentrations of **TNT.**

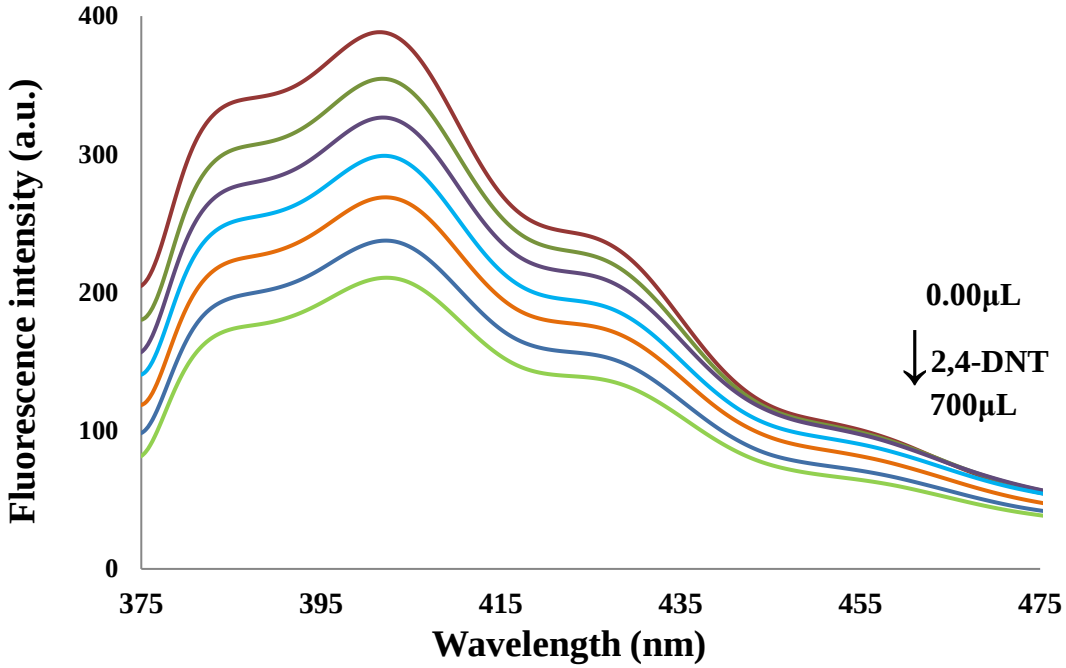

Figure S20.Fluorescence emission spectra of **TMU-21(L2)** dispersed in toluene solution at different concentrations of **2,4-DNT.**

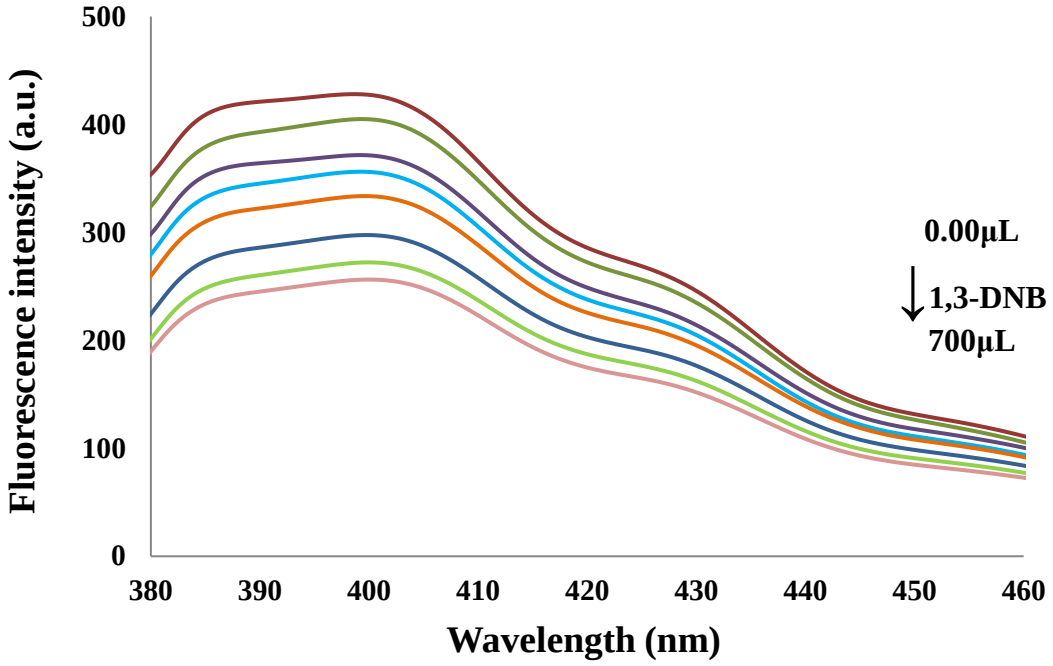

Figure S21.Fluorescence emission spectra of **TMU-21(L2)** dispersed in toluene solution at different concentrations of **1,3-DNB.**

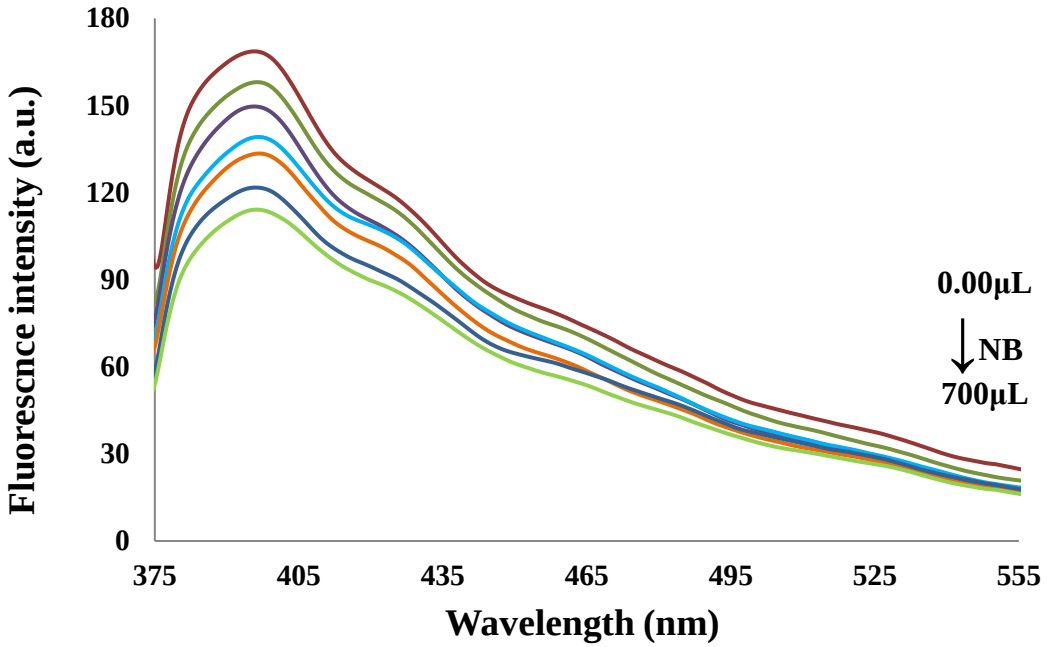

Figure S22.Fluorescence emission spectra of **TMU-21(L2)** dispersed in toluene solution at different concentrations of **NB**

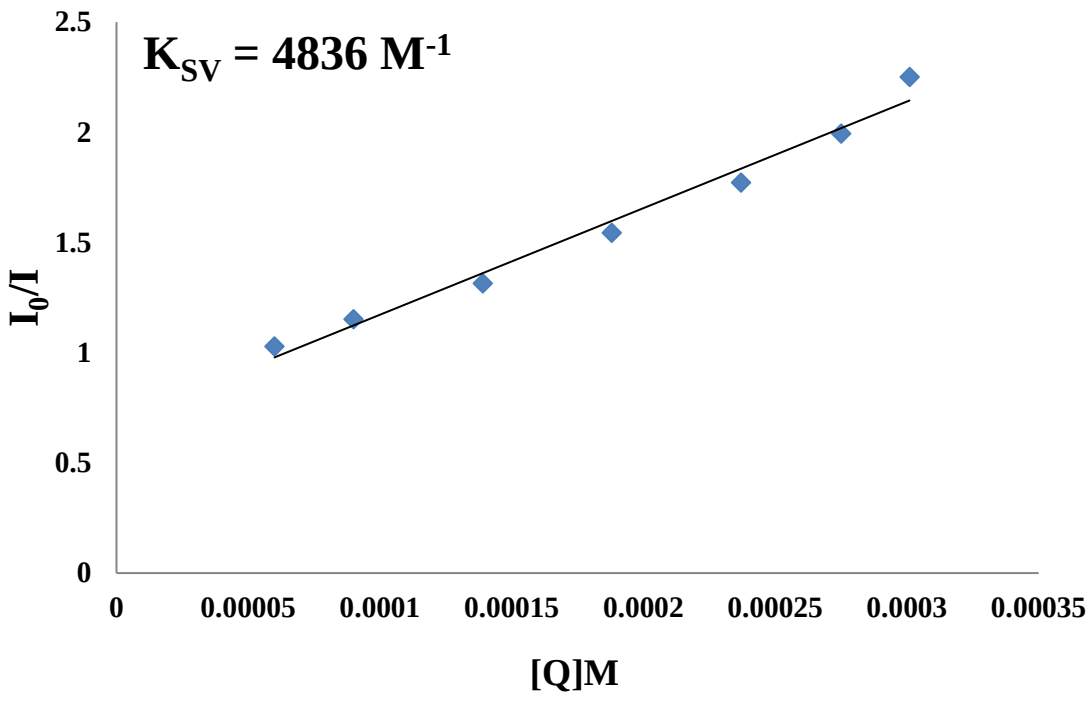
K_{SV} = 4836 M^{-1}
2.5
2
1.5
1
0.5
0
I_0/I
0
0.00005
0.0001
0.00015
0.0002
0.00025
0.0003
0.00035
[Q]M

(a)

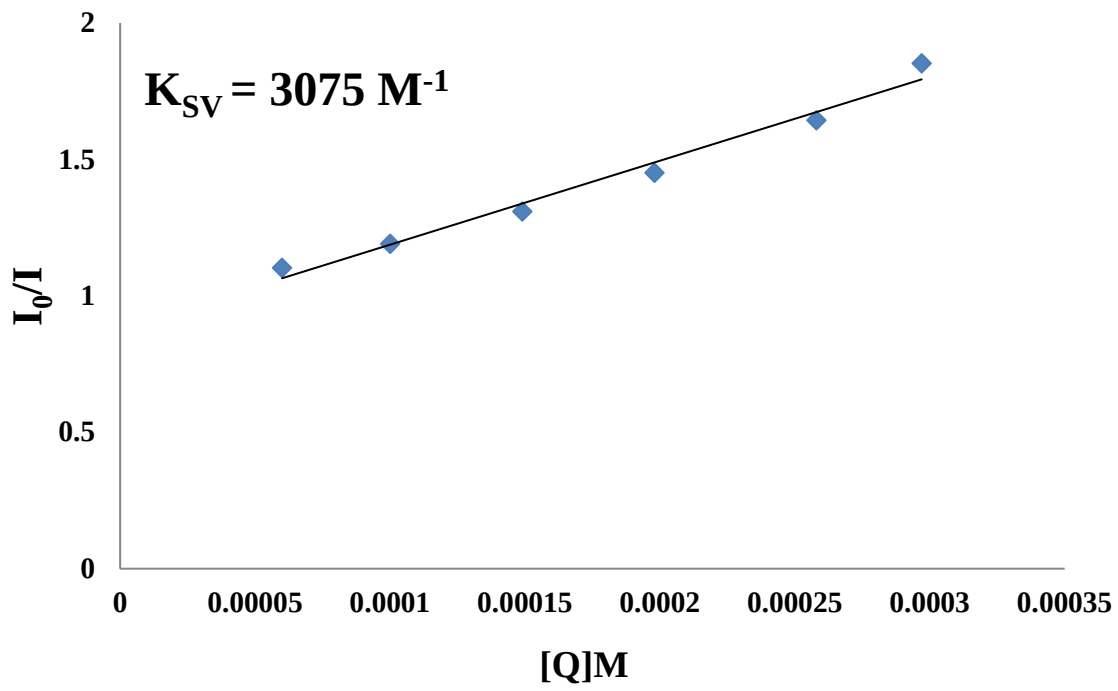
K_{SV} = 3075 M^{-1}
2
1.5
1
0.5
0
I_0/I
0
0.00005
0.0001
0.00015
0.0002
0.00025
0.0003
0.00035
[Q]M

(b)

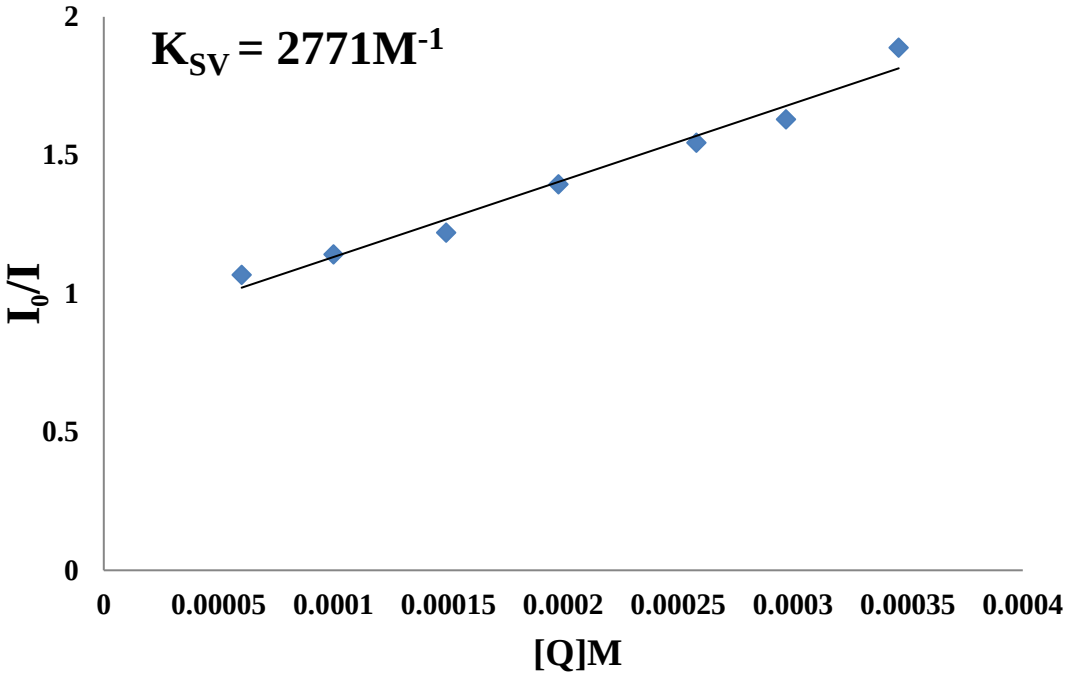

(c)

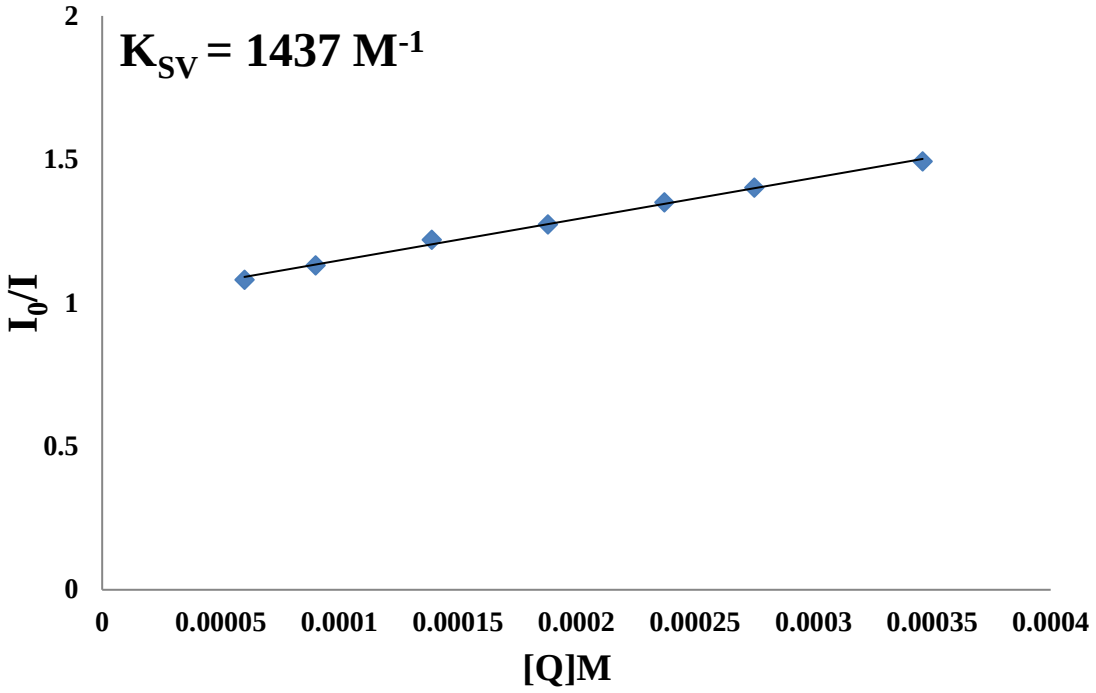

(d)

Figure S23.Stern -Volmer (SV) plots in the presence of 2 mg of **TMU-21(L2)** in different **TNT** (a) **2,4-DNT** (b) **1,3-DNB** (c) **NB** (d) concentrations ([Q]) in toluene.

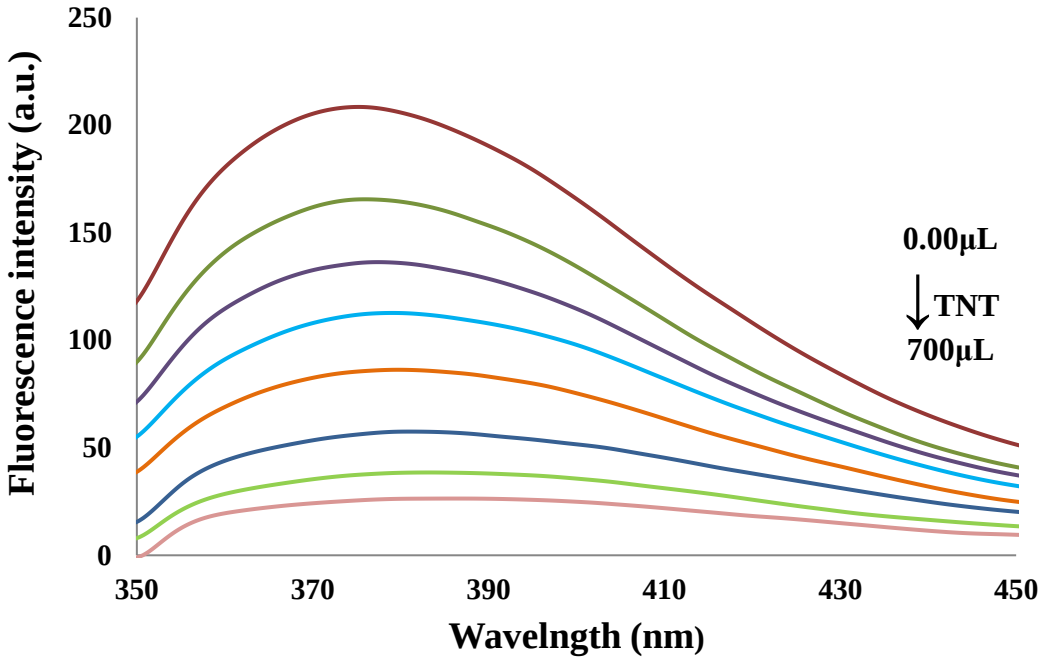

Figure S24.Fluorescence emission spectra of **TMU-6(RL1)** dispersed in toluene solution at different concentrations of **TNT.**

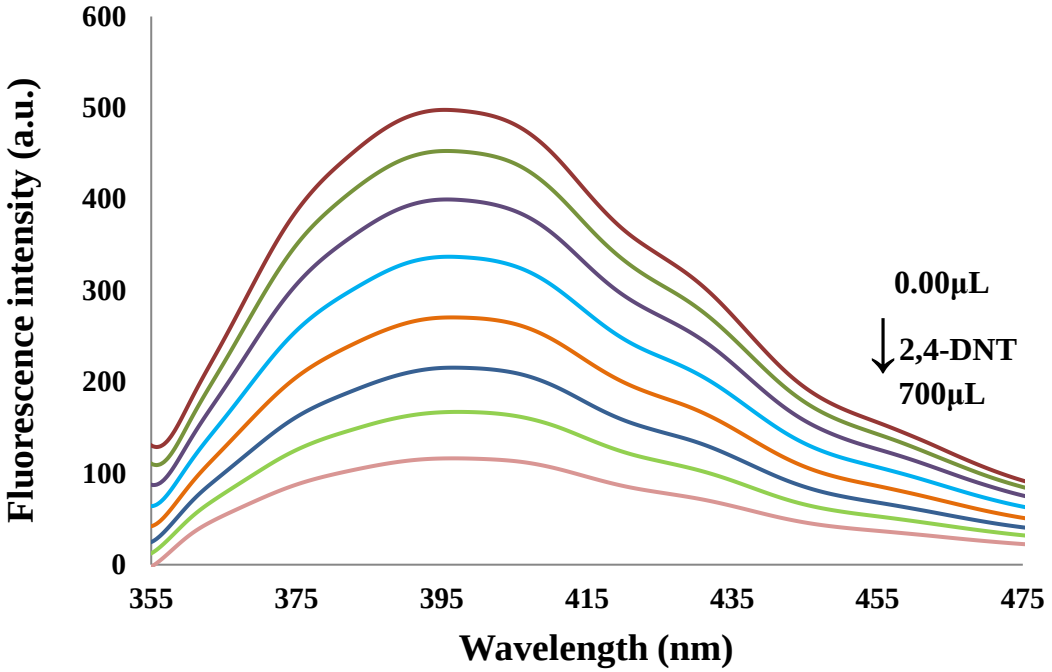

Figure S25.Fluorescence emission spectra of **TMU-6(RL1)** dispersed in toluene solution at different concentrations of **2,4-DNT.**

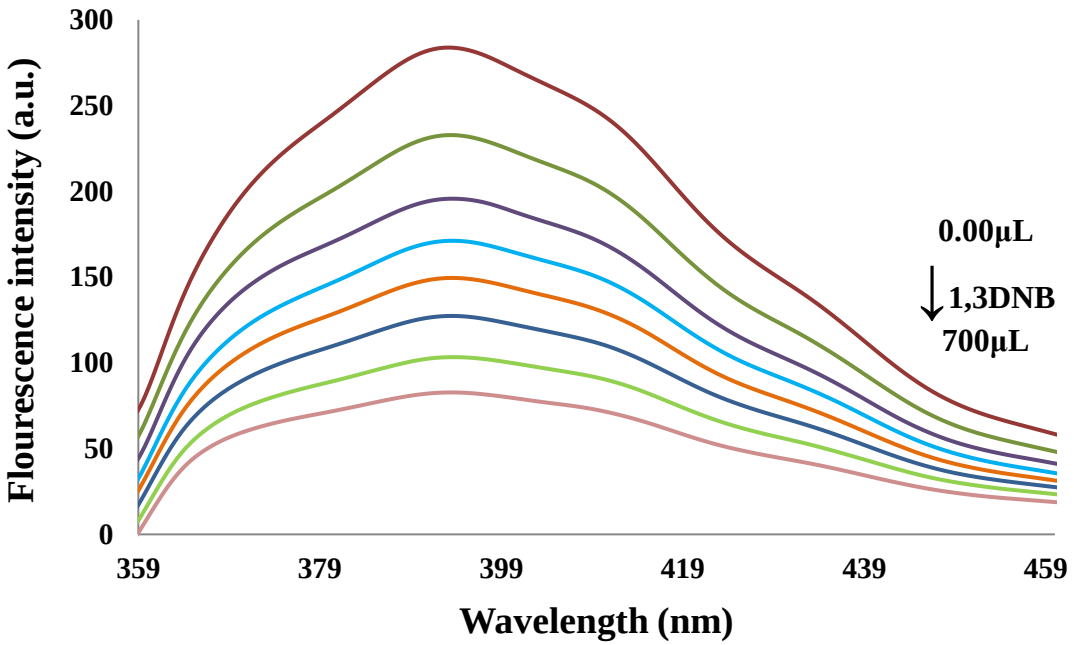

Figure S26.Fluorescence emission spectra of **TMU-6(RL1)** dispersed in toluene solution at different concentrations of **1,3-DNB.**

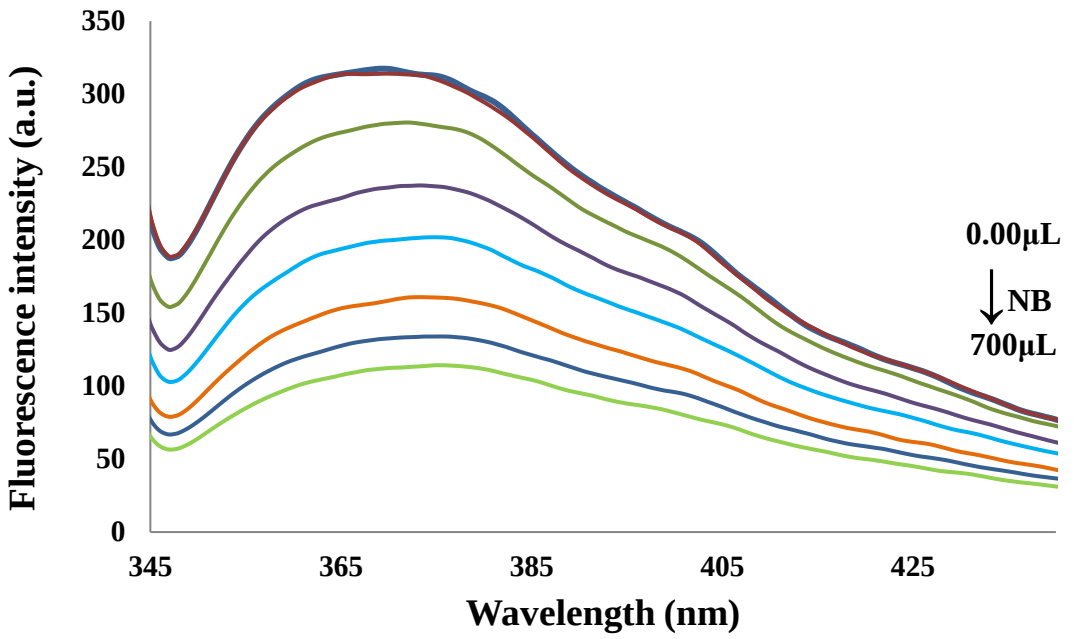

Figure S27.Fluorescence emission spectra of **TMU-6(RL1)** dispersed in toluene solution at different concentrations of **NB.**

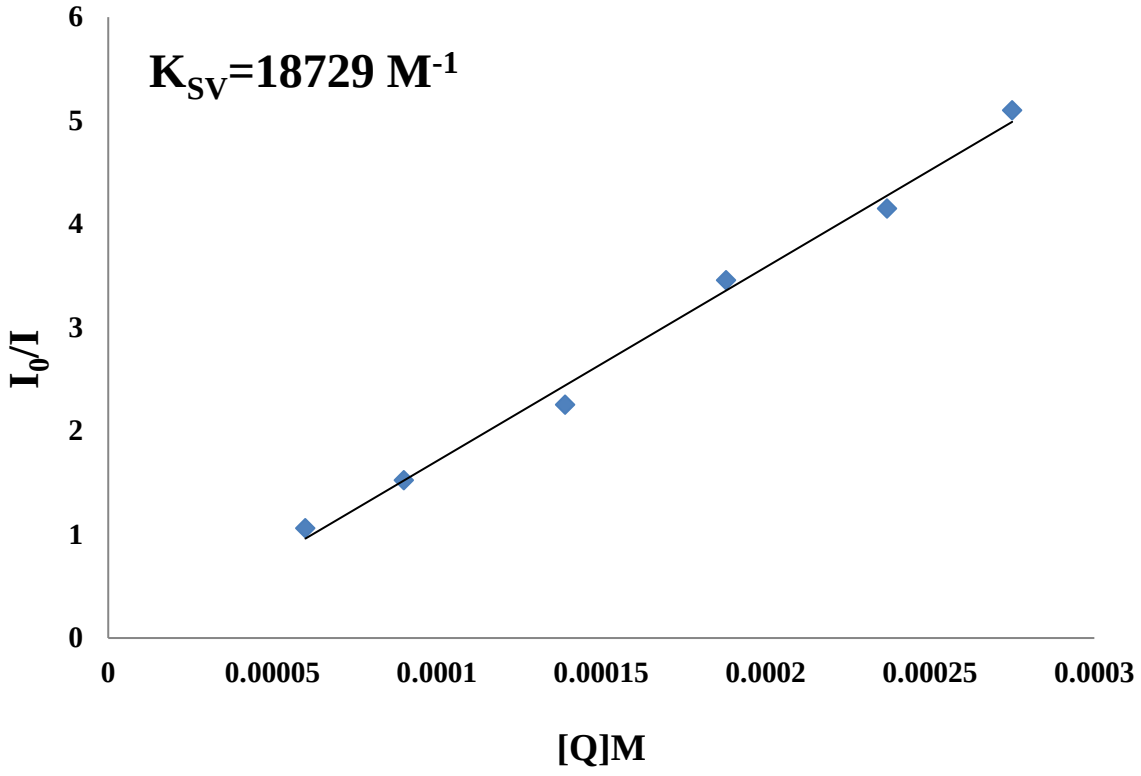
K_{SV}=18729 M^{-1}
I_0/I
0
1
2
3
4
5
6
0
0.00005
0.0001
0.00015
0.0002
0.00025
0.0003
[Q]M

(a)

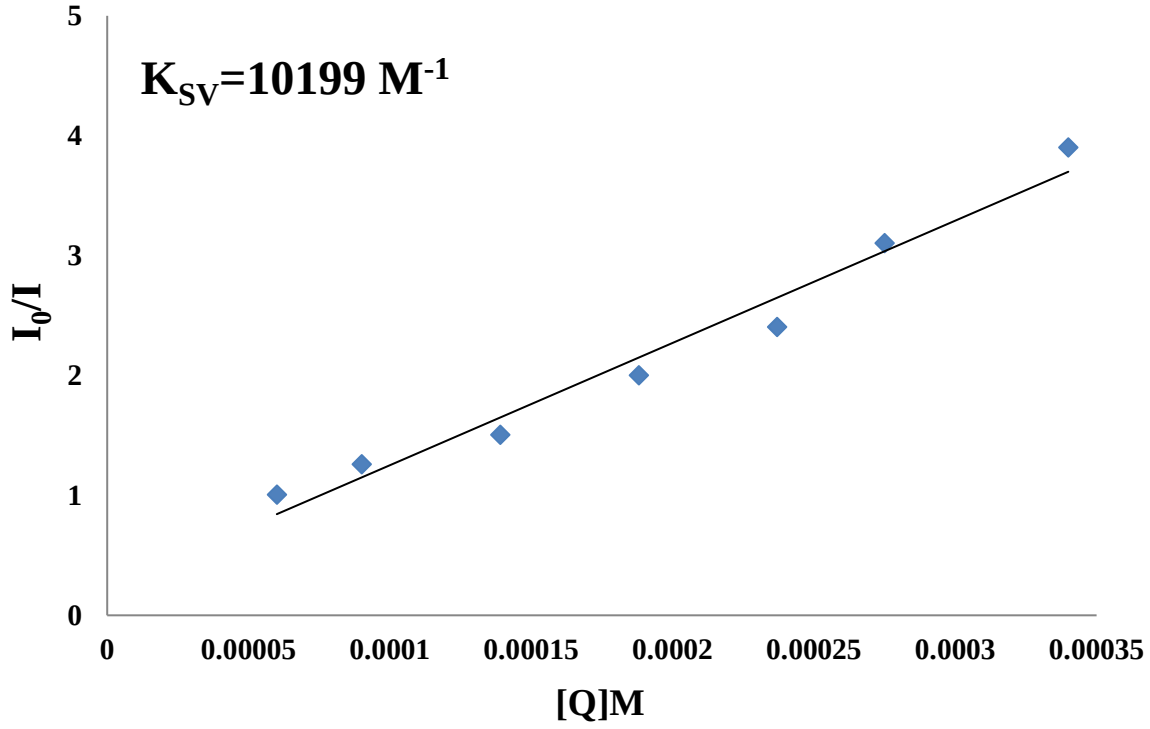
K_{SV}=10199 M^{-1}
I_0/I
0
1
2
3
4
5
0
0.00005
0.0001
0.00015
0.0002
0.00025
0.0003
0.00035
[Q]M

(b)

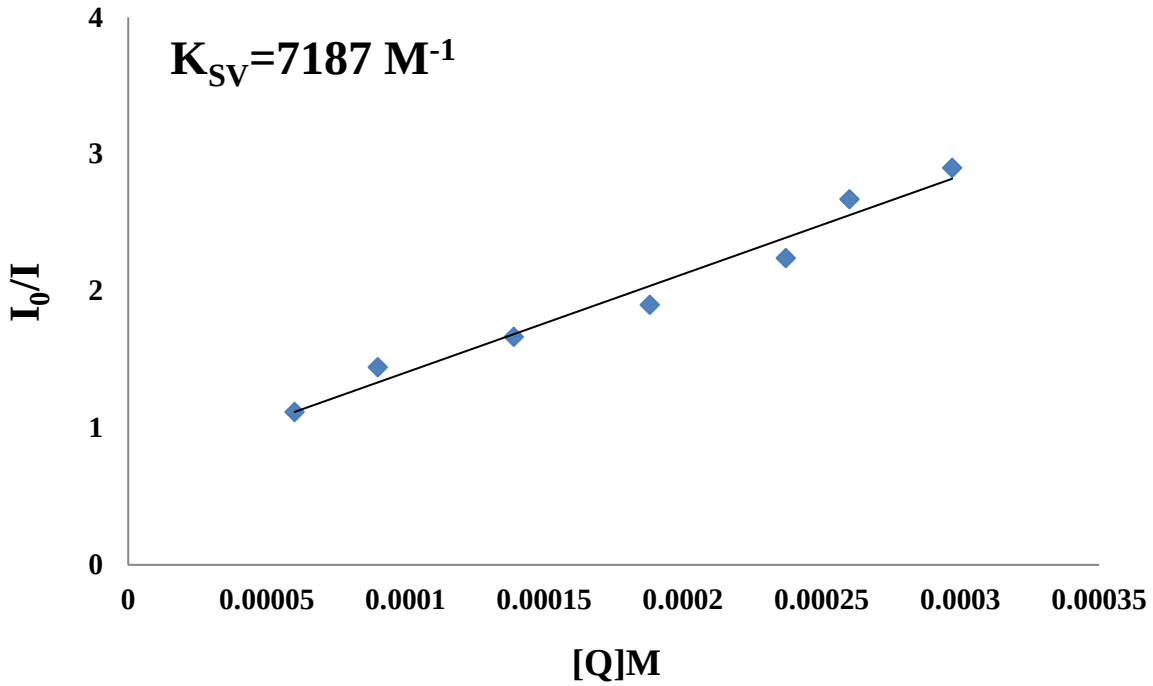

(c)

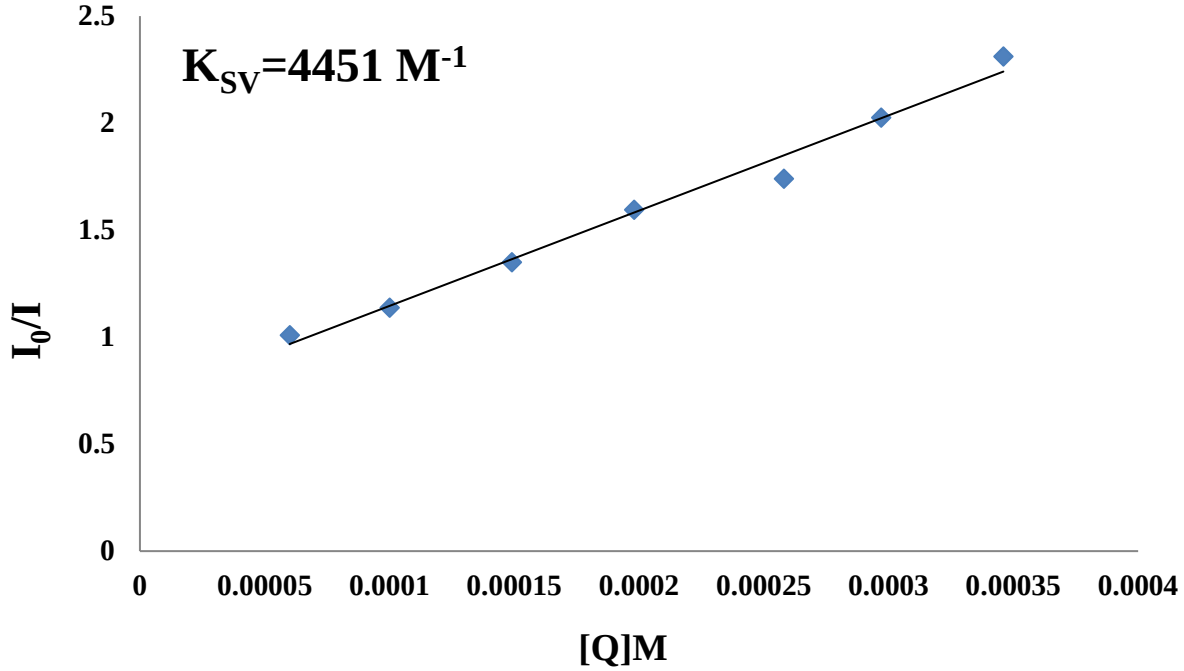

(d)

Figure S28. Stern -Volmer (SV) plots in the presence of 2 mg of **TMU-6(RL1)** in different **TNT** (a) **2,4-DNT** (b) **1,3-DNB** (c) **NB** (d) concentrations ([Q]) in toluene.

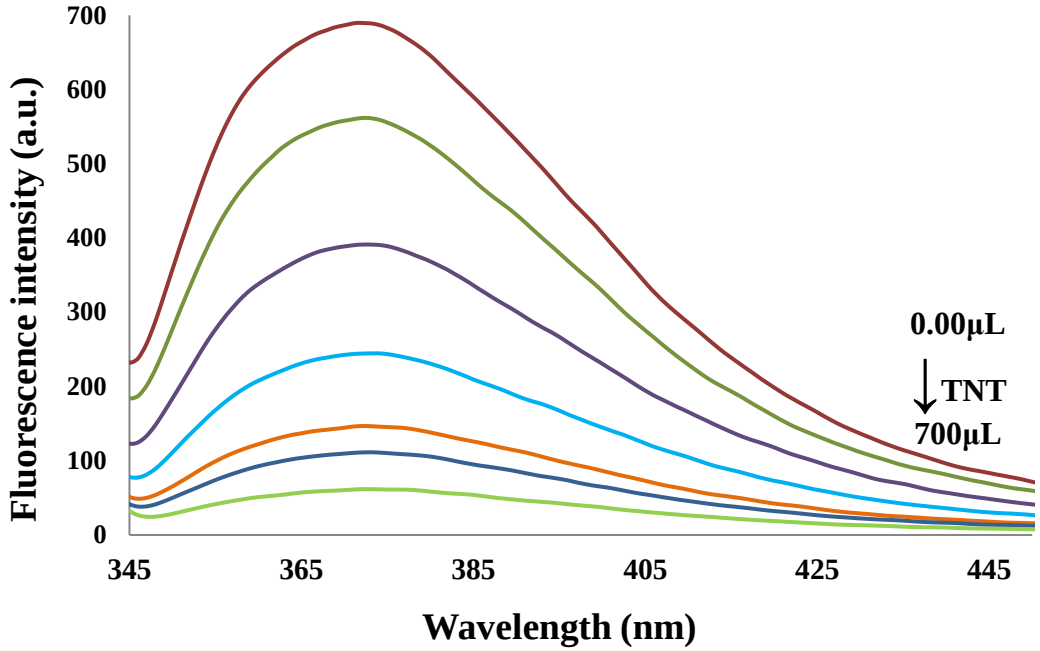

Figure S29.Fluorescence emission spectra of **TMU-21(RL2)** dispersed in toluene solution at different concentrations of **TNT.**

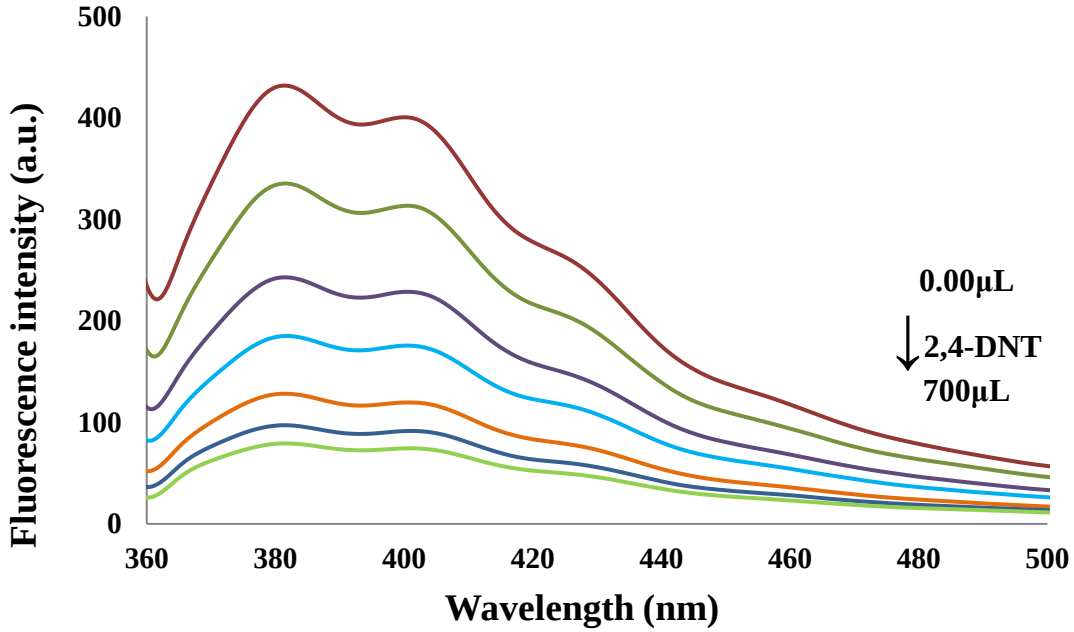

Figure S30.Fluorescence emission spectra of **TMU-21(RL2)** dispersed in toluene solution at different concentrations of **2,4-DNT.**

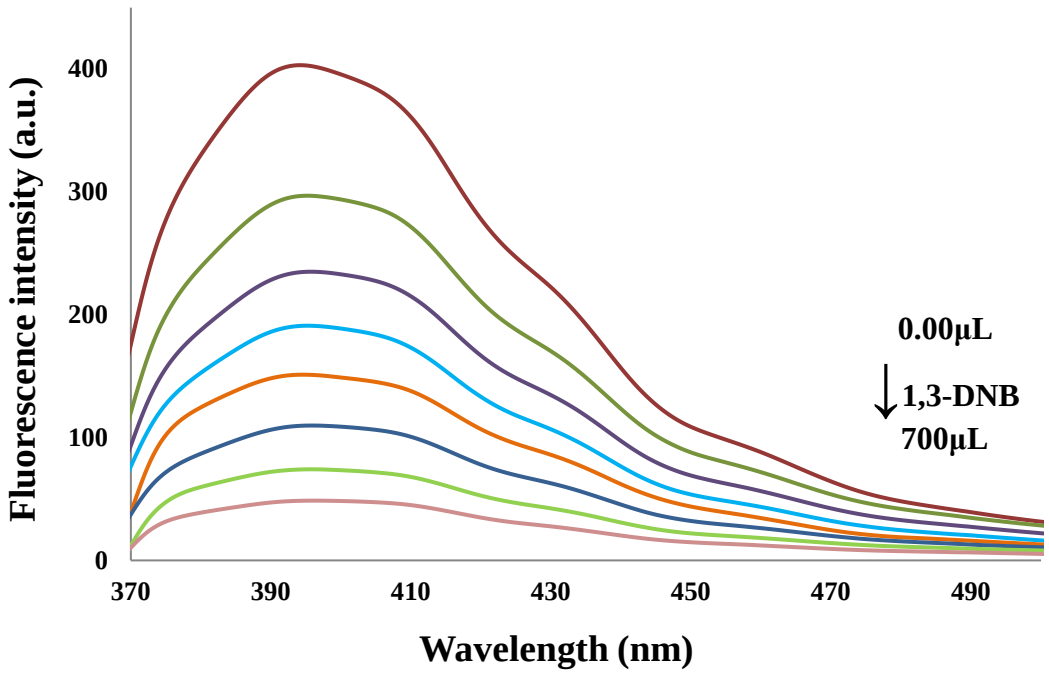

Figure S31.Fluorescence emission spectra of **TMU-21(RL2)** dispersed in toluene solution at different concentrations of **1,3DNB.**

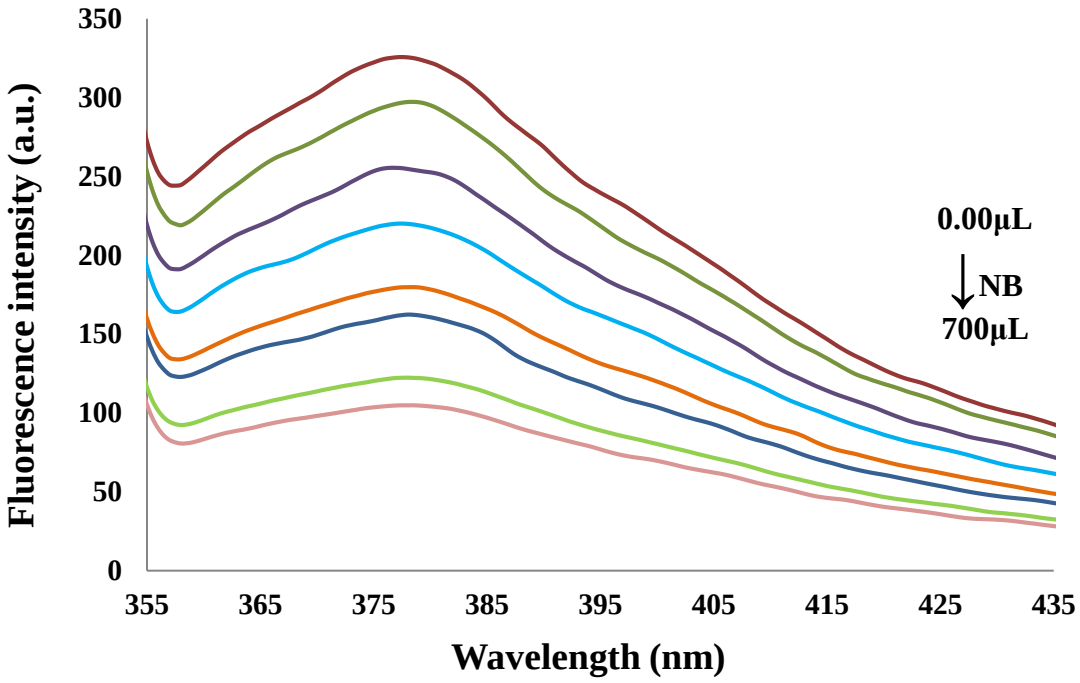

Figure S32.Fluorescence emission spectra of **TMU-21(RL2)** dispersed in toluene solution at different concentrations of **NB.**

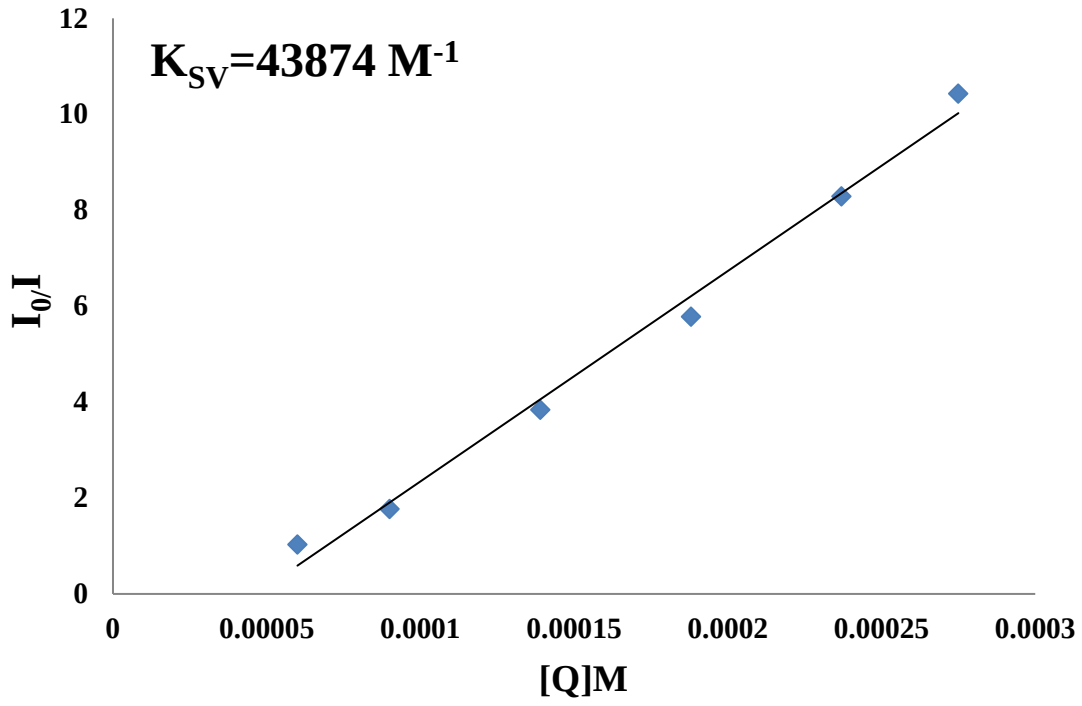
K_{SV}=43874 M^{-1}
12
10
8
6
4
2
0
I_0/I
0
0.00005
0.0001
0.00015
0.0002
0.00025
0.0003
[Q]M

(a)

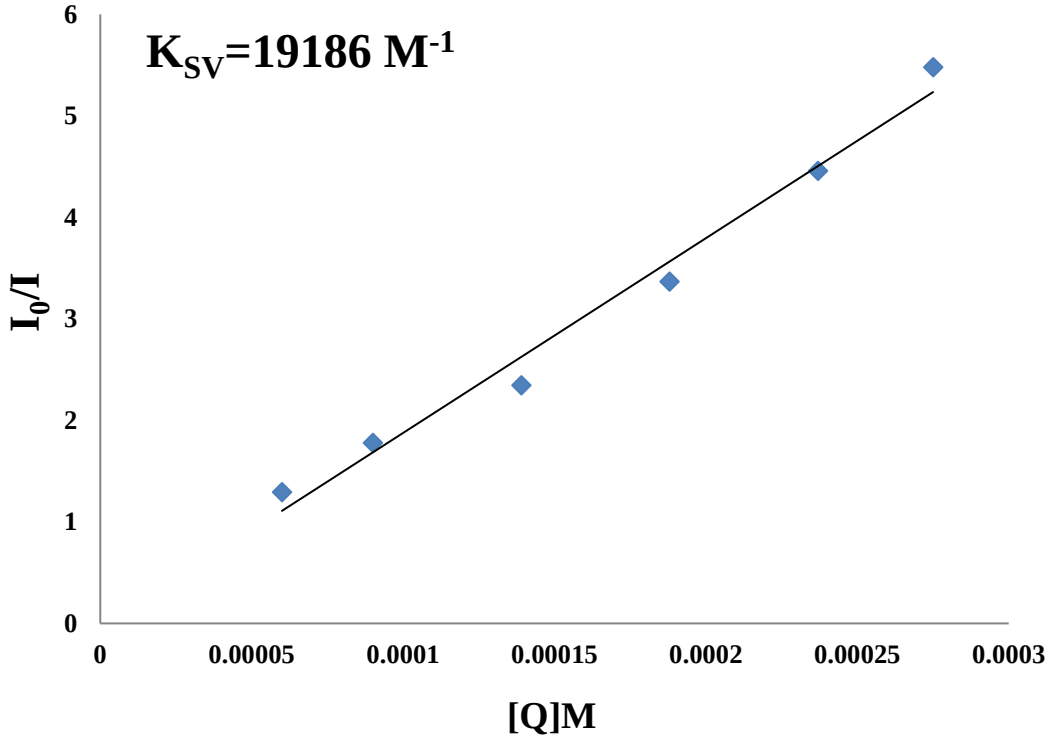
K_{SV}=19186 M^{-1}
6
5
4
3
2
1
0
I_0/I
0
0.00005
0.0001
0.00015
0.0002
0.00025
0.0003
[Q]M

(b)

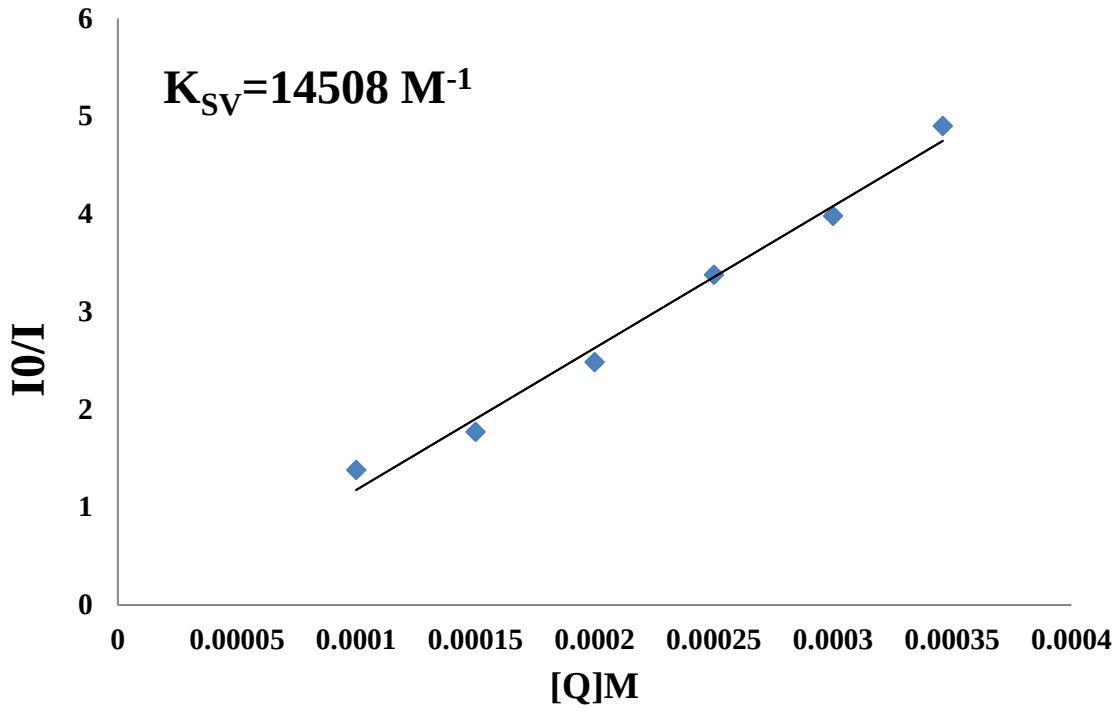

(c)

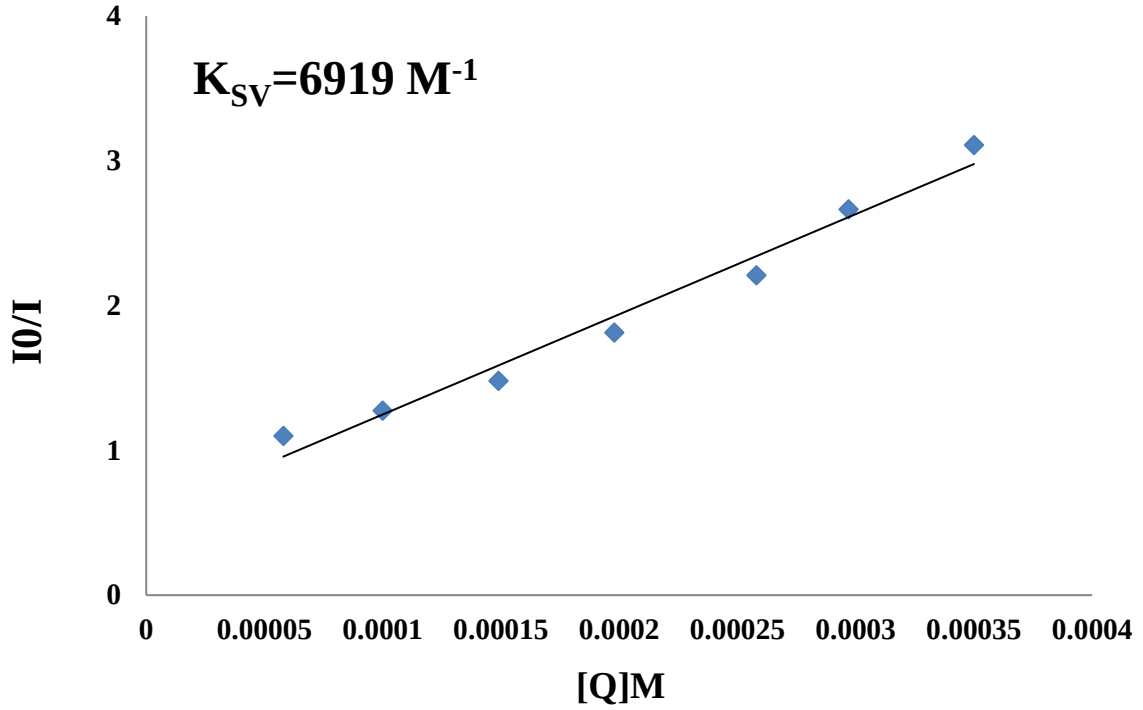

(d)

Figure S33. Stern -Volmer (SV) plots in the presence of 2 mg of **TMU-21(RL2)** in different **TNT** (a) **2,4-DNT** (b) **1,3-DNB** (c) **NB** (d) concentrations ([Q]) in toluene.

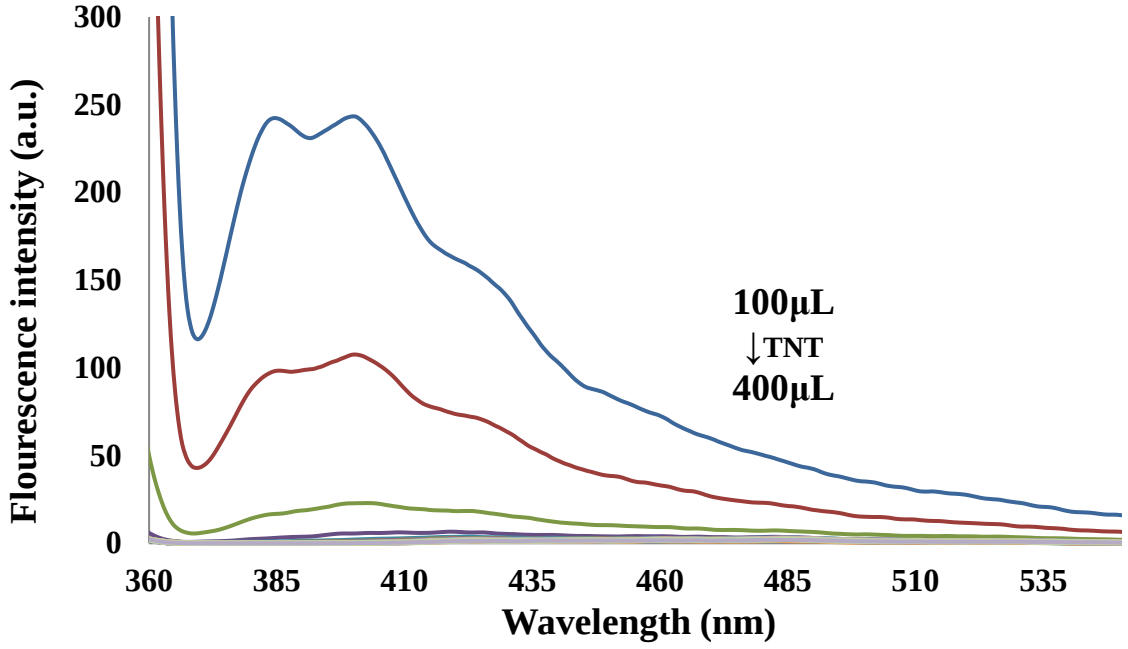

Figures 34. Fluorescence emission spectra of **TMU-21(RL2)** dispersed in toluene solution at .01-.05 M concentration of **TNT.**

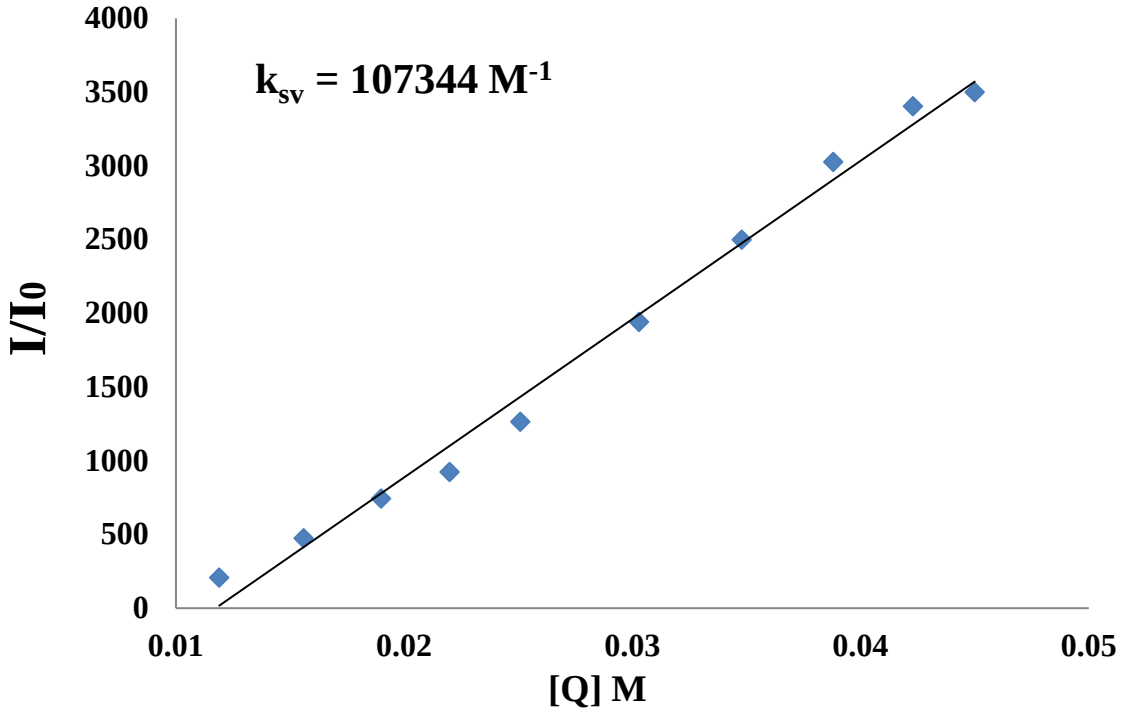

Figure S35. Stern -Volmer (SV) plots in the presence of 2 mg of **TMU-21(RL2)** in different **TNT** concentrations ([Q]) in toluene.

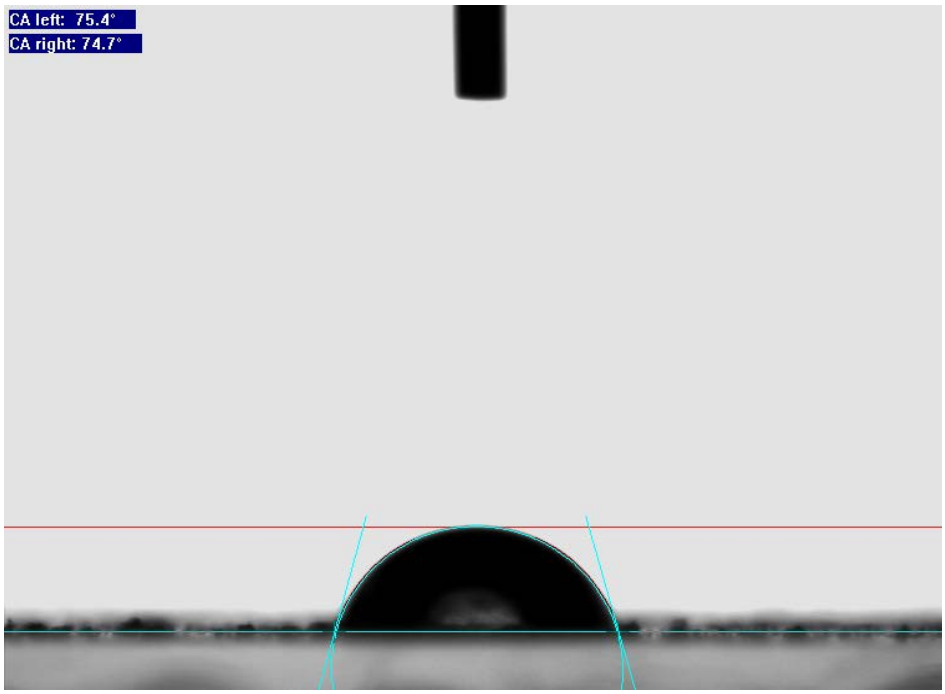

Figure S36. Contact angles of **TMU-21(L2)**

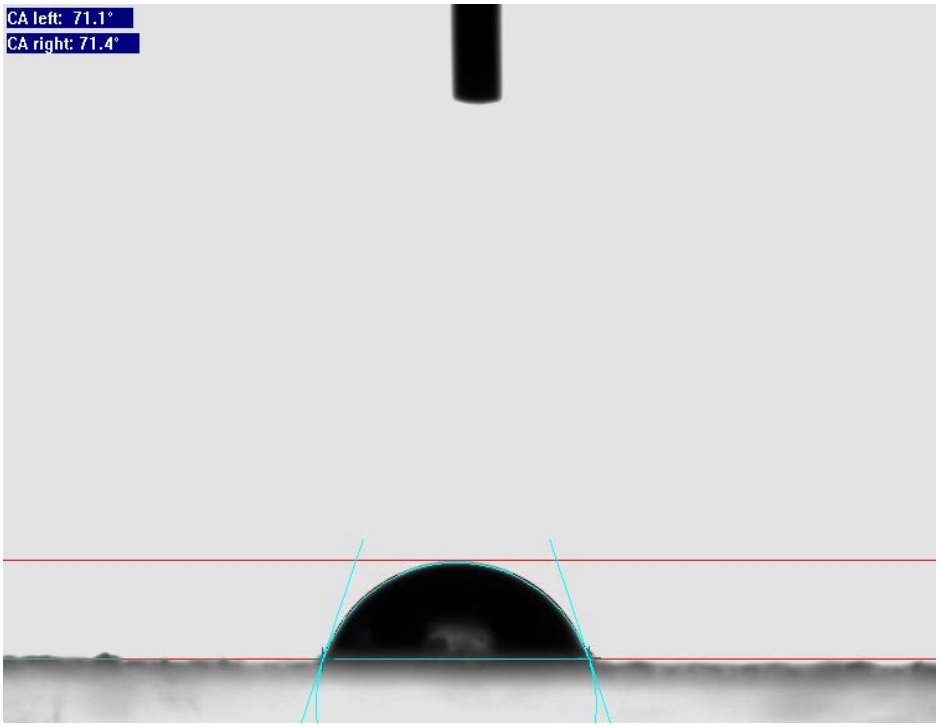

Figure S37. Contact angles of **TMU-21(RL2)**

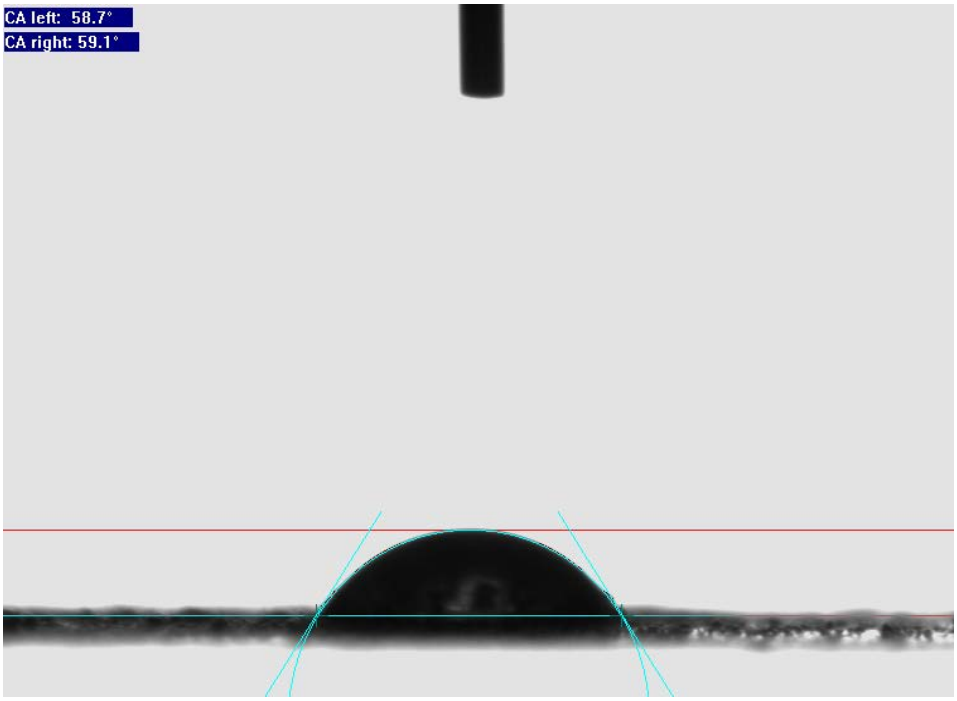

Figure S38. Contact angles of **TMU-6(RL1)**

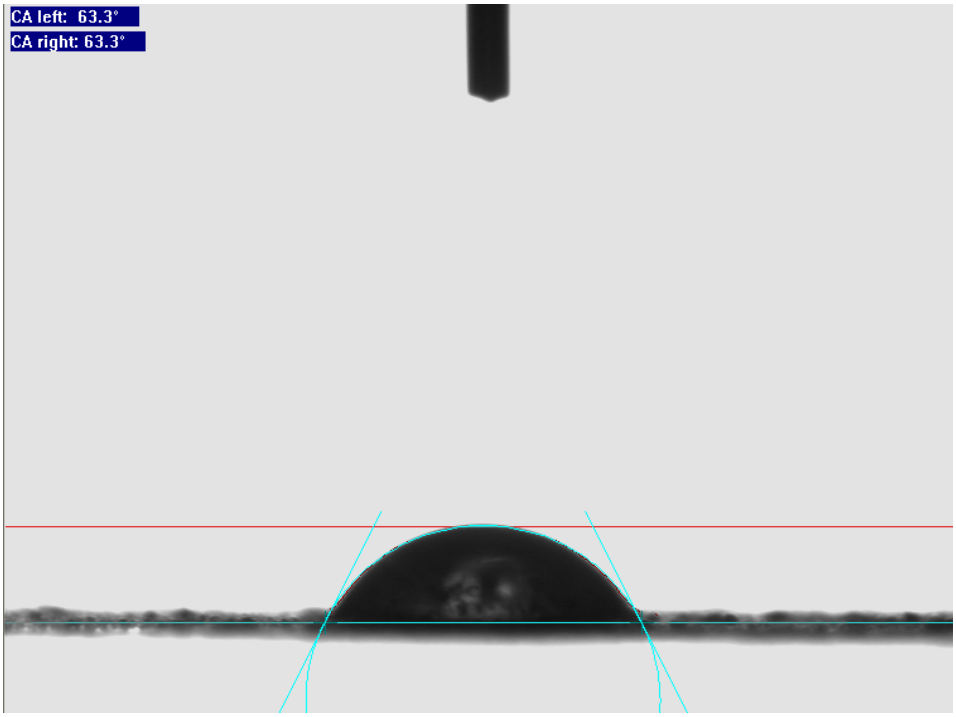

Figure S39. Contact angles of **TMU-6(L1)**

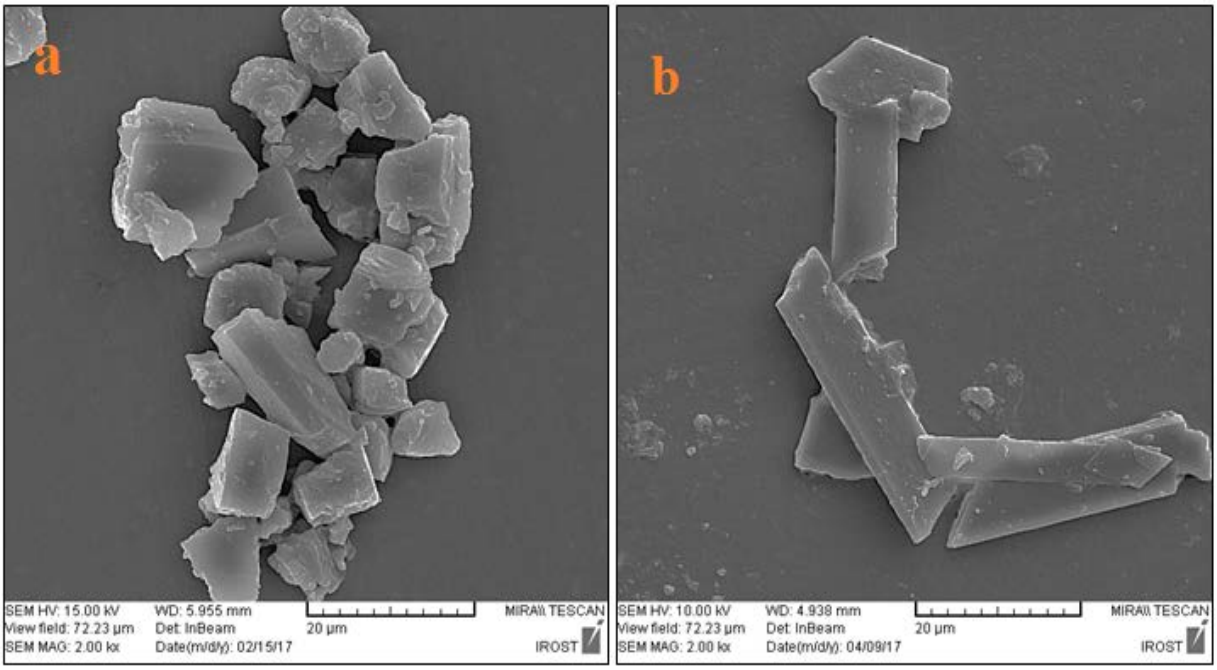

Figure S40. FE-SEM images of **TMU-6(L1)** as-synthesized particles (a) after sensing (b)

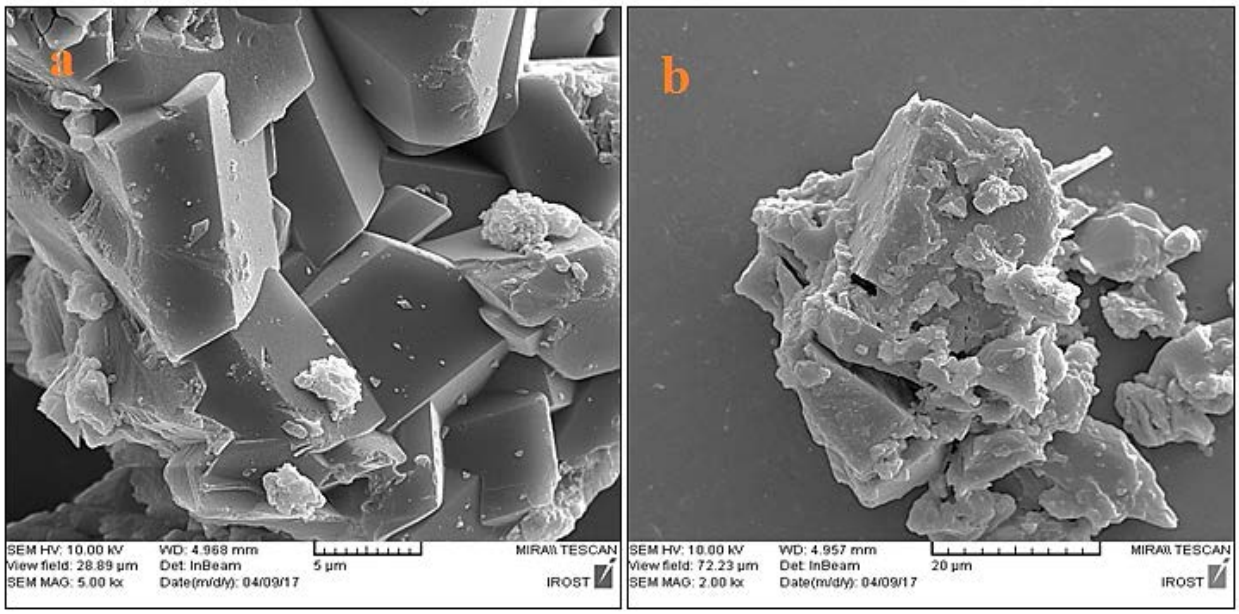

Figure S41. FE-SEM images of **TMU-21(L2)** as-synthesized particles (a) after sensing (b)

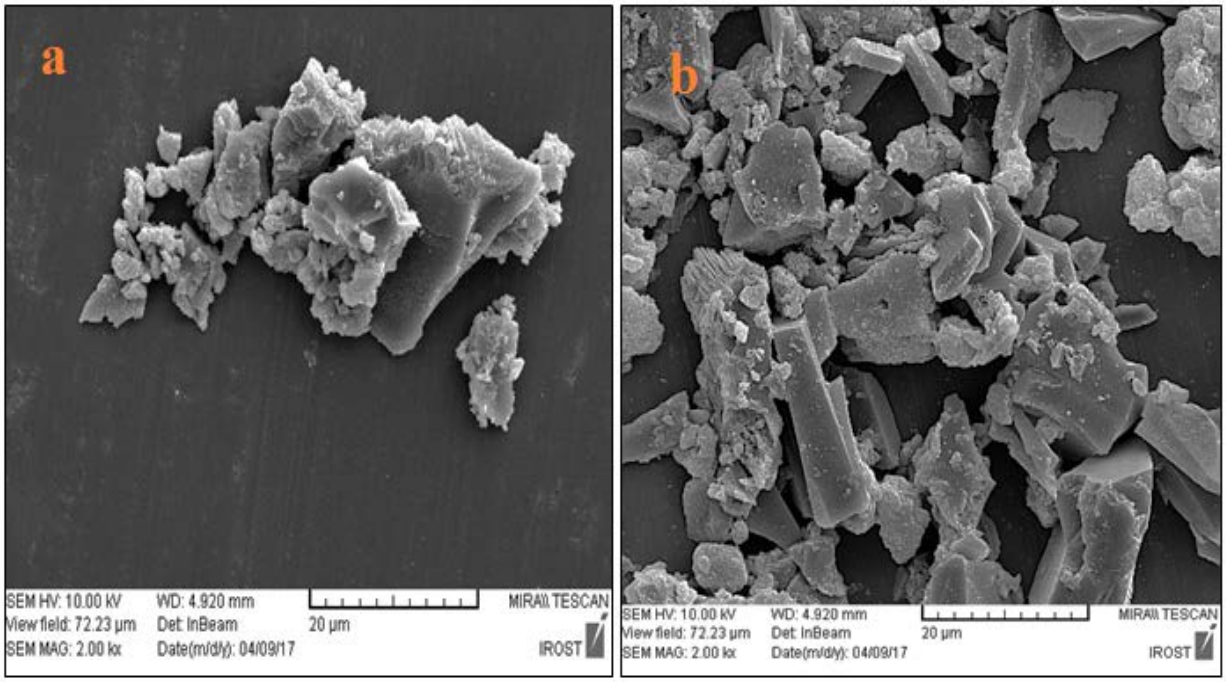

Figure S42. FE-SEM images of **TMU-6(RL1)** as-synthesized particles (a) after sensing (b)

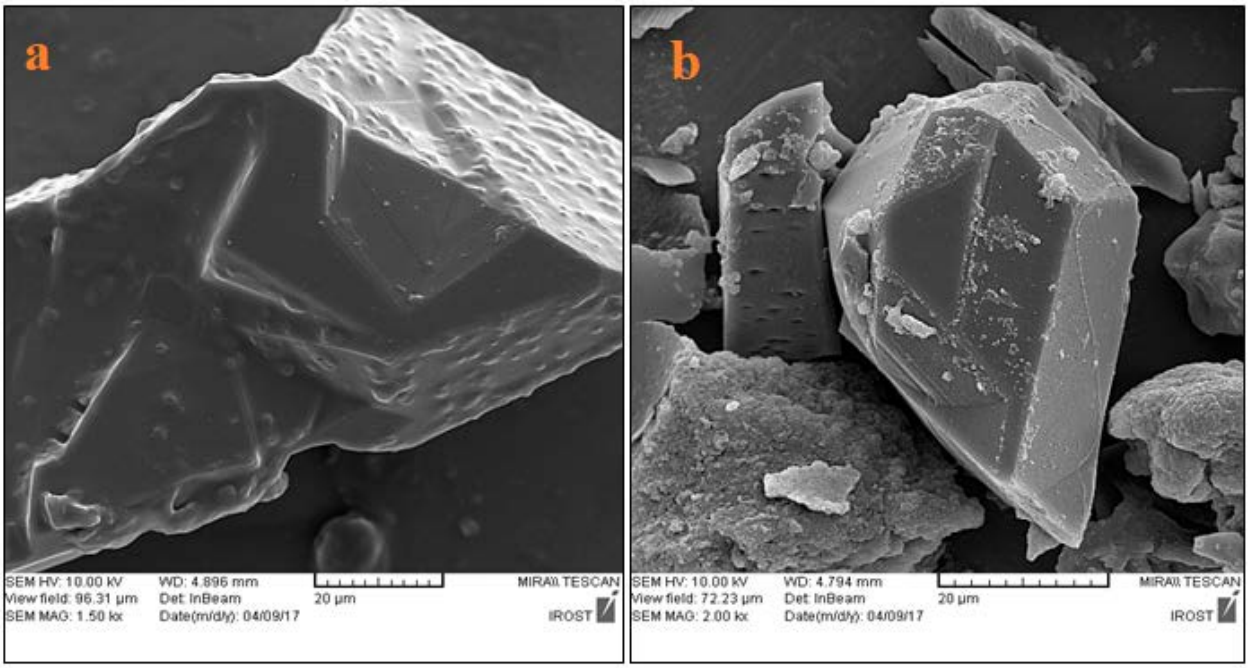

Figure S43. FE-SEM images of **TMU-21(RL1)** as-synthesized particles (a) after sensing (b)

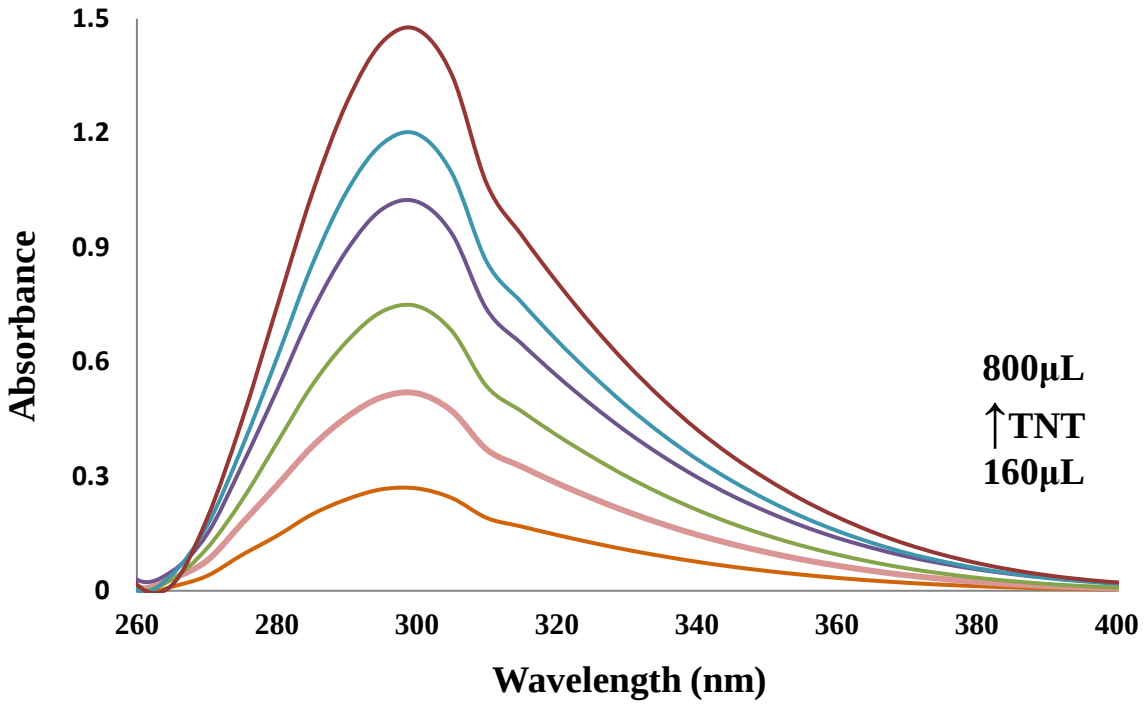

Figure S44. UV-vis spectra of different concentrations of TNT.

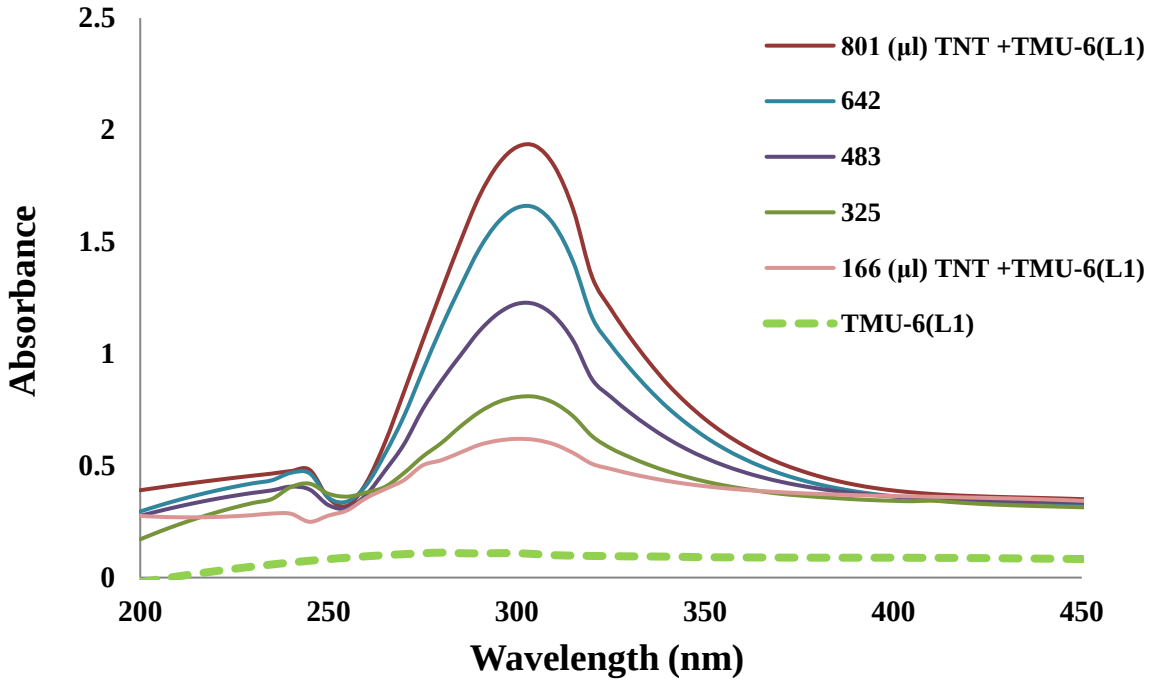

Figure S45. UV-vis spectra of different concentrations (µl) of TNT in the presence of TMU-6(L1).

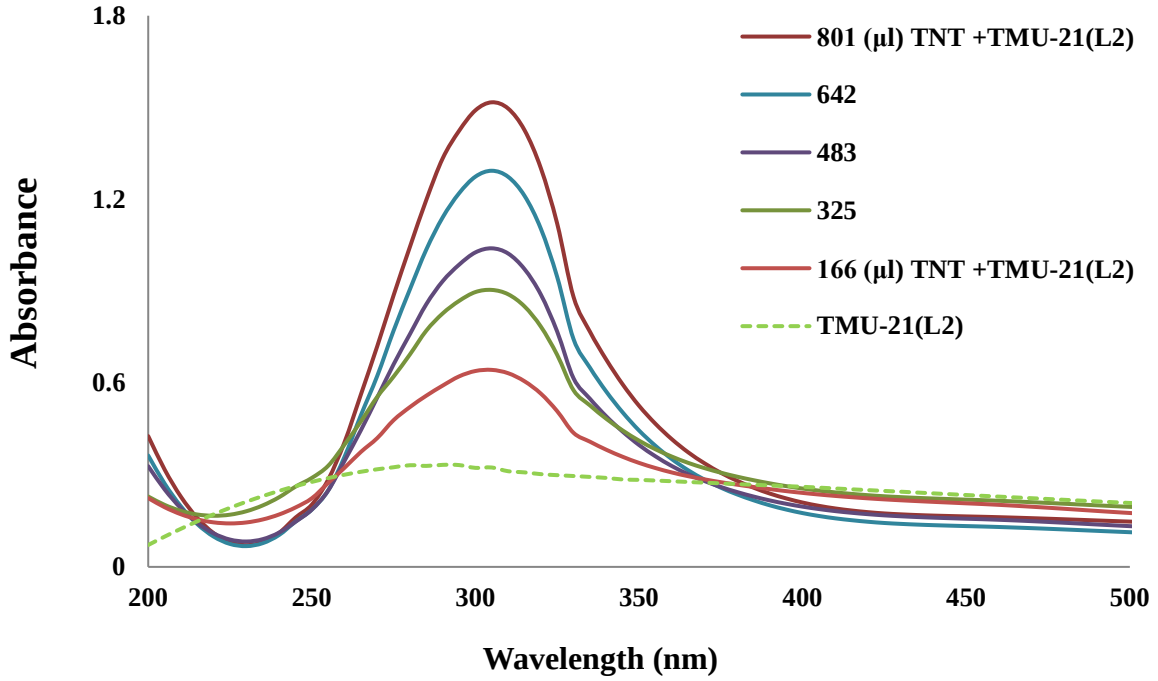

Figure S46. UV-vis spectra of different concentrations (µl) of TNT in the presence of TMU-21(L2).

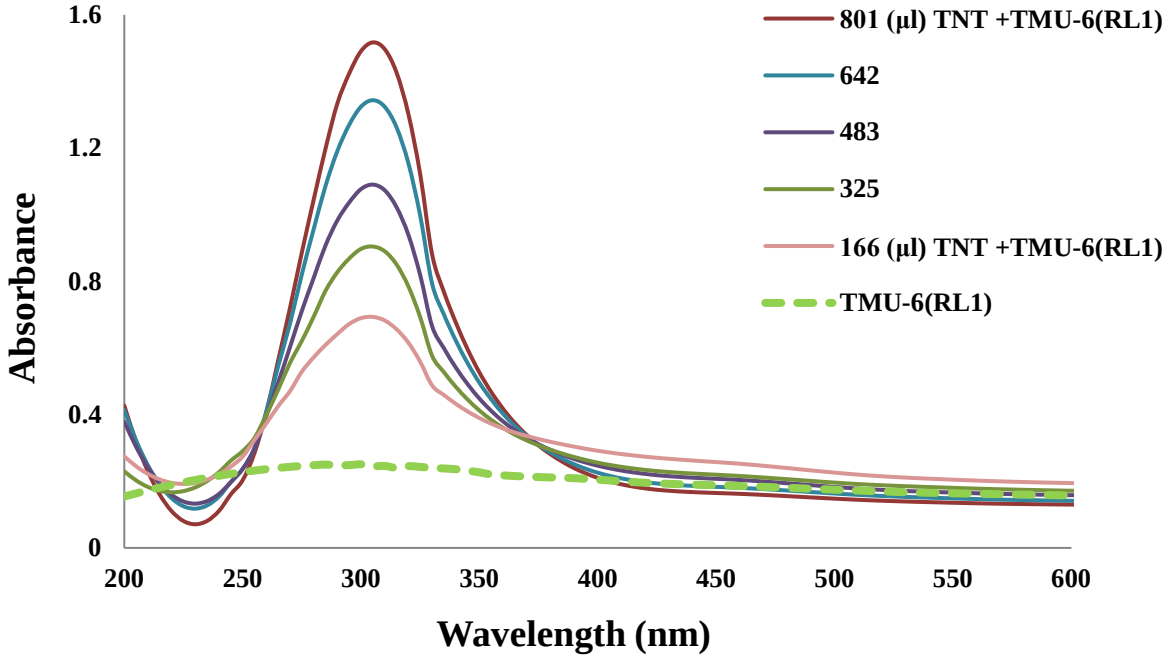

Figure S47. UV-vis spectra of different concentrations (µl) of TNT in the presence of TMU-6(RL1).

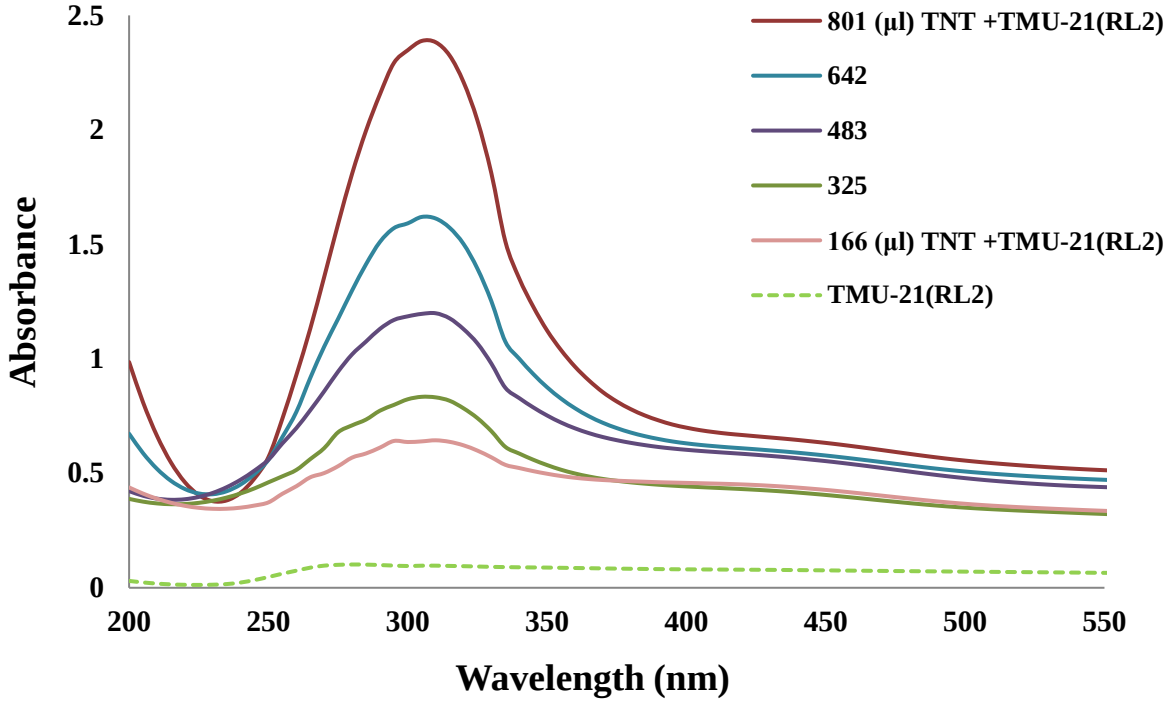

Figure S48. UV-vis spectra of different concentrations (µl) of TNT in the presence of TMU-21(RL2).

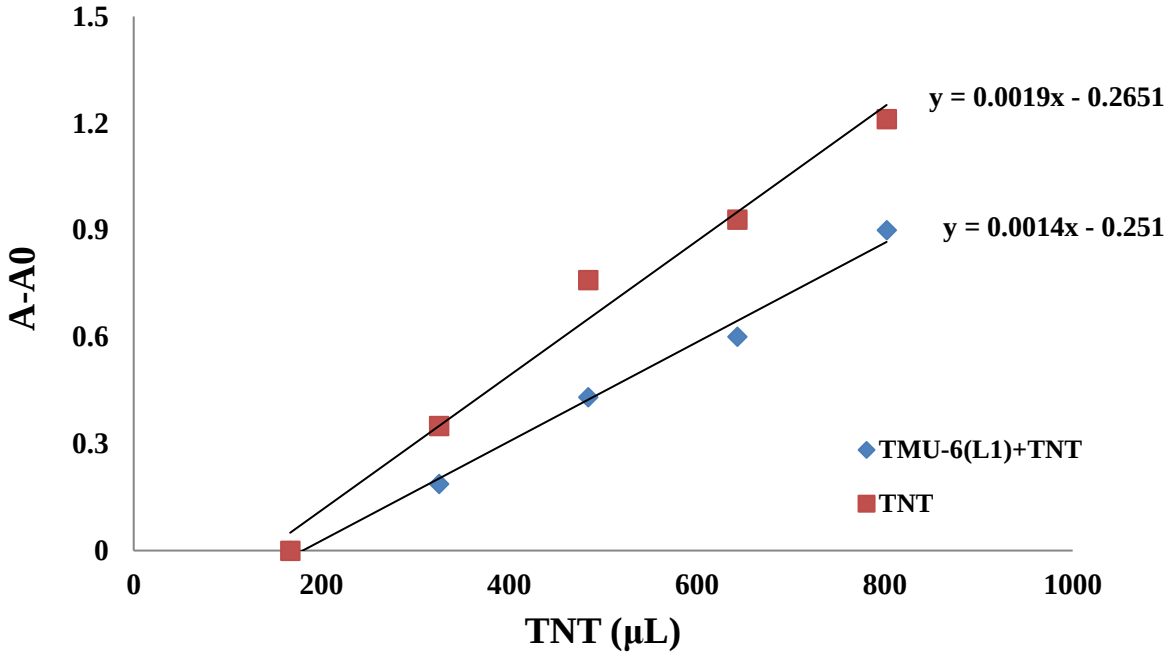

(a)

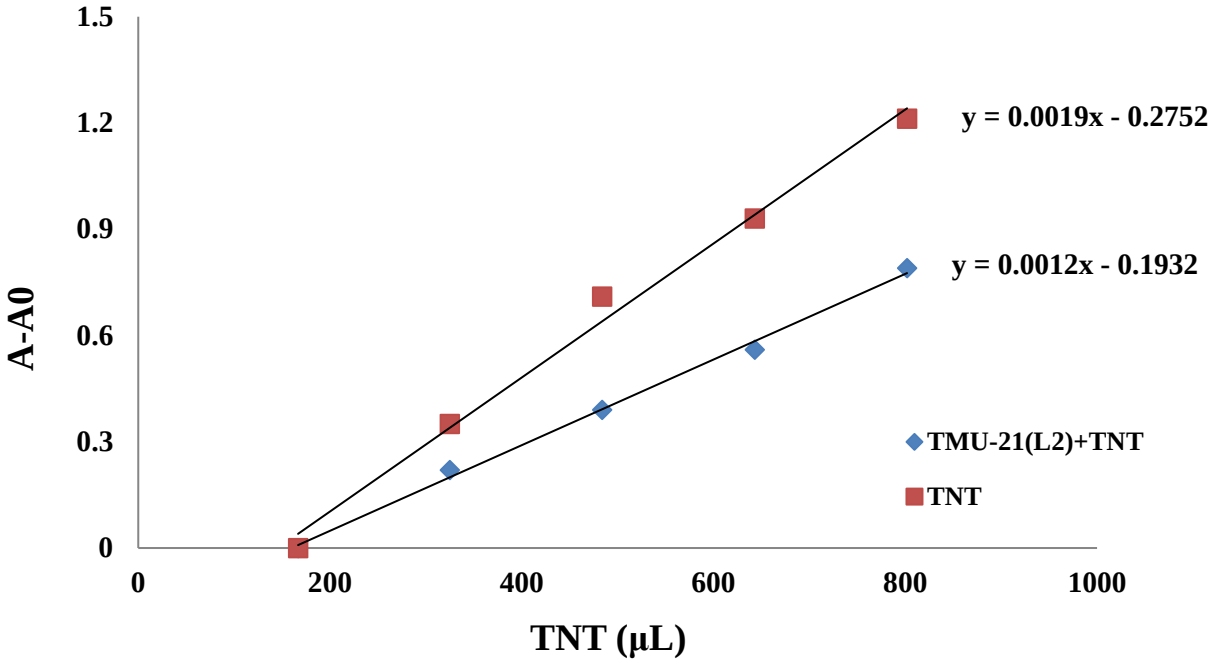

(b)

Figure S49. The changes in absorbance at 300 nm upon addition of different concentrations of TNT in the presence and absence of a) TMU-6(L1) and b) TMU-21(L2) in toluene.

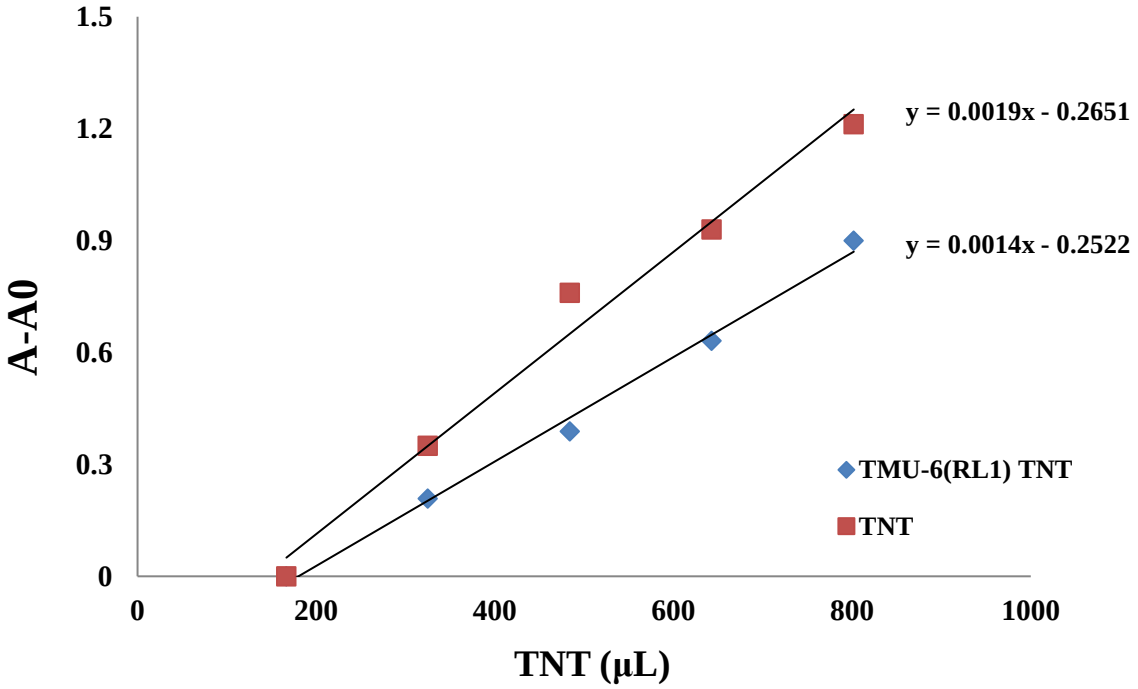

(a)

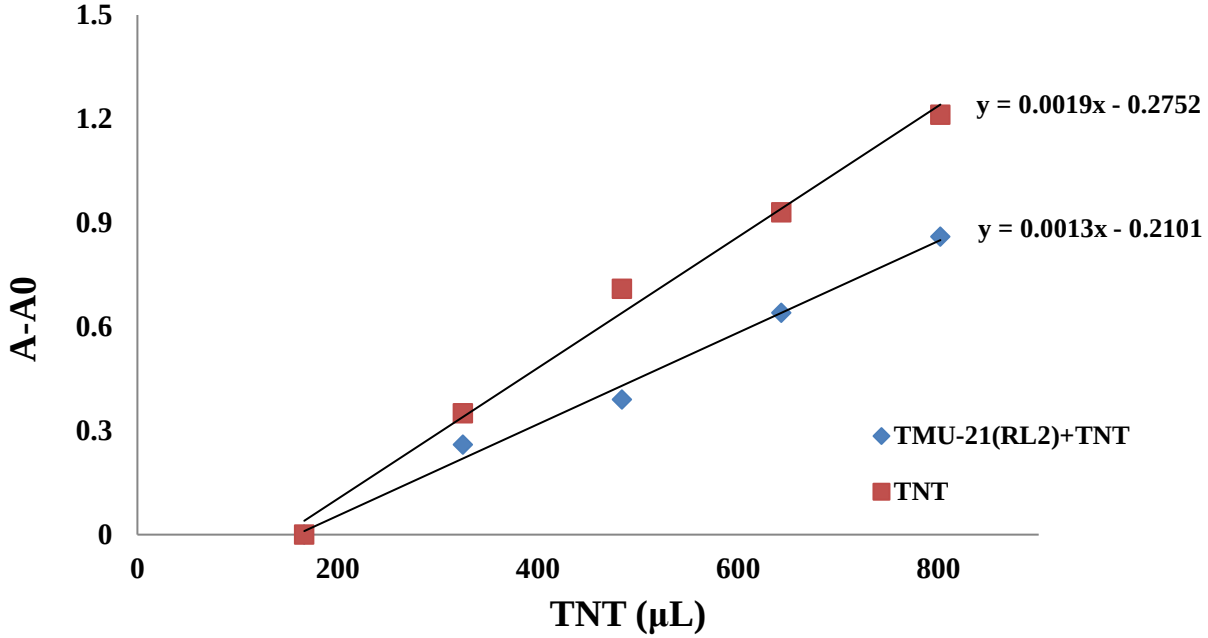

(b)

Figure S50. The changes in absorbance at 300 nm upon addition of different concentrations of TNT in the presence and absence of a) TMU-6(RL1) and b) TMU-21(RL2) in toluene.

Table **S1.** Relative contributions of various non-covalent contacts to the Hirshfeld surface area in compounds TMU-6(L1), TMU-6(RL1), TMU-21(L2) and TMU-21(RL2).

Compound	H···H	C···H	C···C	N···H	O···H	Zn···O
TMU-6 (L1)	44.8	18.5	7.5	4.8	12.7	6.4
TMU-6 (RL1)	46.8	18.8	7.1	2.1	15.3	5.9
TMU-21 (L2)	46.2	18.7	9.9	2.1	13.1	5.5
TMU-21 (RL2)	47.8	19.4	7.0	1.9	14.0	5.5

Extraction Procedure

To approve diffusion of aromatic compounds to the frameworks' pores, at first 10 mL toluene solution including 300 ppb of TNT, was added to 3 mg of the MOFs as sorbent. After stirring for 20 min in order to enhance the speed of adsorption, The MOFs was separated from the samples by centrifugation and then washed with methanol to remove the physically adsorbed species on the MOFs surface. The analytes were desorbed from the sorbent with 1 mL of methanol by powerful vortex for 5 minutes. The extracts were further concentrated under a gentle stream of nitrogen gas to 100 µl prior to GC-MS analysis and analyzed by GC-MASS.

Table S2. Comparison of LOD and quenching constant of the proposed method and other techniques indetermination of TNT

Probes	Material	LDO (nM)	K_{SV} (M^{-1})	Reference
Molecularly imprinted polymer	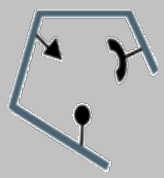	40700	------	1
graphene quantum dots (GQDs) from GO	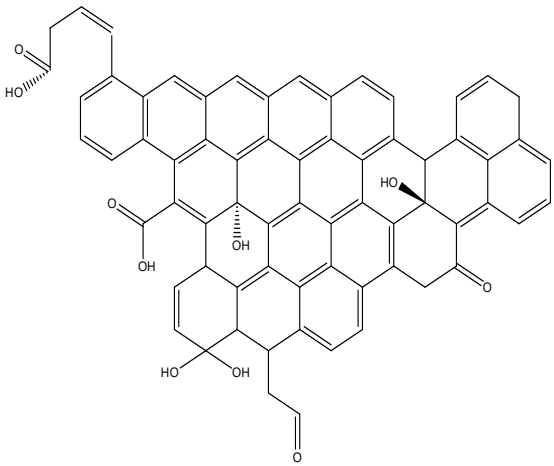	2200	8×10^3	2
Cross-linking electropolymerized films -TCPC	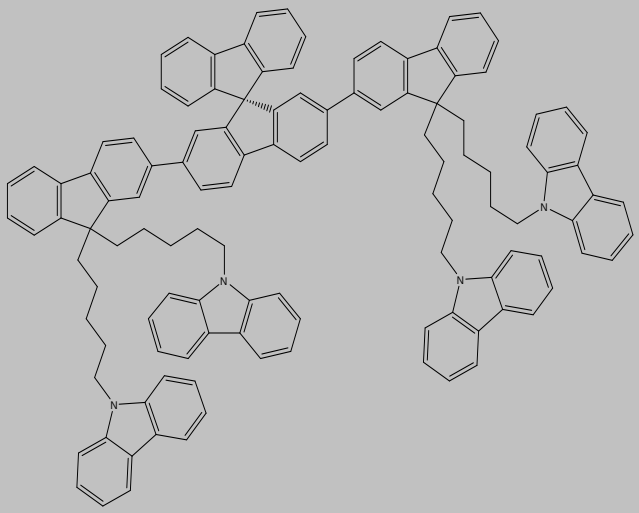 TCPC	10000	1.6×10^3	3

Probes	Material	LDO (nM)	K_{SV} (M^{-1})	Reference
Phenylethynylene calix[4]arenes -ANC	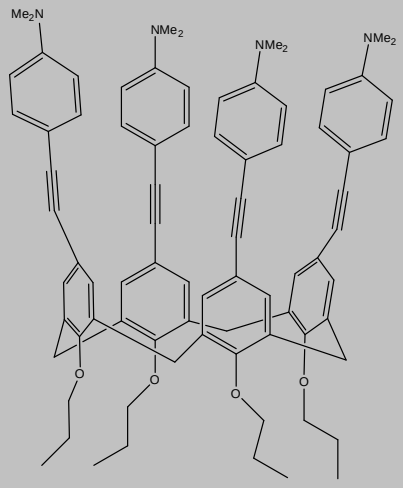 **ANC**	**300**	**1.09×10^{5}**	**4**
Metal–organic frameworks **(PCN-224)** **Zr6(OH)8 ,TCPC**	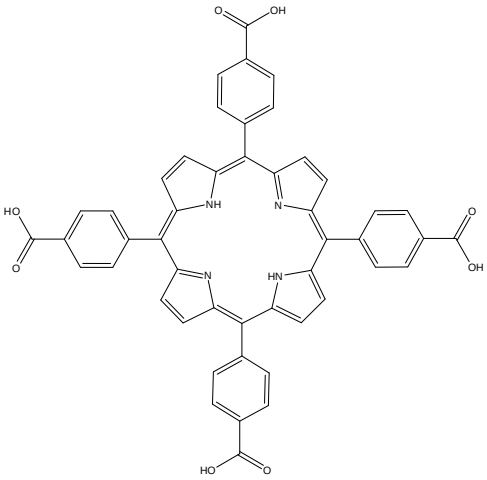 **TCPC** 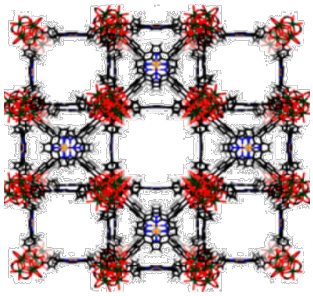 **(PCN-224)**	**460**	**3.5×10^{4}**	**5**

Probes	Material	LDO (nM)	K_{SV} (M^{-1})	Reference
Water-soluble pyrene derivatives	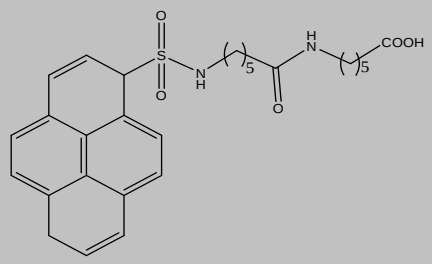 6-(6-(1-Pyrenesulfamido)hexanamide) hexanoic acid	801	3.3×10^4	6
Water soluble conjugated polymer nanoparticles (N-methylpolypyrrole-SDBS)	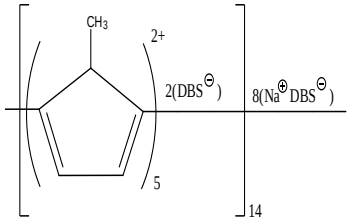 NMPPY-SDBS	100	3.5×10^4	7
Metal–organic frameworks TMU-21(RL2) RL2,Oba,Zn	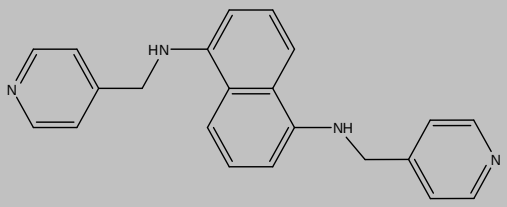 RL2 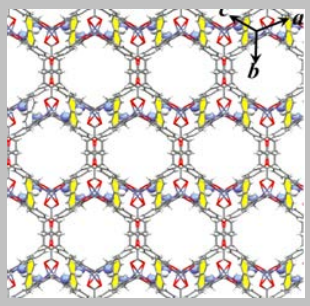 TMU-21(RL2)	112	4.3×10^4	This Work

Reference

1. R. C. Stringer, S. Gangopadhyay and S. A. Grant, *Analytical Chemistry*, 2010, **82**, 4015-4019.
2. L. Fan, Y. Hu, X. Wang, L. Zhang, F. Li, D. Han, Z. Li, Q. Zhang, Z. Wang and L. Niu, *Talanta*, 2012, **101**, 192-197.
3. H. Nie, Y. Lv, L. Yao, Y. Pan, Y. Zhao, P. Li, G. Sun, Y. Ma and M. Zhang, *Journal of Hazardous Materials*, 2014, **264**, 474-480.
4. K. Boonkitpatarakul, Y. Yodta, N. Niamnont and M. Sukwattanasinitt, *RSC Advances*, 2015, **5**, 33306-33311.
5. J. Yang, Z. Wang, K. Hu, Y. Li, J. Feng, J. Shi and J. Gu, *ACS Applied Materials & Interfaces*, 2015, **7**, 11956-11964.
6. I. S. Kovalev, O. S. Taniya, N. V. Slovesnova, G. A. Kim, S. Santra, G. V. Zyryanov, D. S. Kopchuk, A. Majee, V. N. Charushin and O. N. Chupakhin, *Chemistry – An Asian Journal*, 2016, **11**, 775-781.
7. N. Alizadeh, A. Akbarinejad and A. Ghoorchian, *ACS Applied Materials & Interfaces*, 2016, **8**, 24901-24908.